



REPUBLIC OF TÜRKİYE
ALTINBAŞ UNIVERSITY
Institute of Graduate Studies
Electrical And Computer Engineering

**LITHIUM ION BATTERY SOLAR CHARGER
DESIGN AND SIMULATION**

Ali Riyadh Abdulmajeed AL-TEKREETI

Master's Thesis

Supervisor

Asst. Prof. Dr. Mesut ÇEVİK

Istanbul, 2022

**LITHIUM ION BATTERY SOLAR CHARGER DESIGN AND
SIMULATION**

ALI RIYADH ABDULMAJEED AL-TEKREETI

Electrical And Computer Engineering

Master's Thesis

ALTINBAŞ UNIVERSITY

2022

The thesis titled LITHIUM ION BATTERY SOLAR CHARGER DESIGN AND SIMULATION prepared by Ali Riyadh Abdulmajeed AL-TEKREETI and submitted on 21/12/2022 has been accepted unanimously for the degree of Master of Science in Electrical And Computer Engineering.

Asst. Prof. Dr. Mesut ÇEVİK

Supervisor

Thesis Defense Committee Members:

Asst. Prof. Dr. Mesut ÇEVİK

Electrical and Electronics
Engineering,

Altınbaş University

Asst. Prof. Dr. Abdullahi IBRAHİM

Department of Computer
Engineering,

Altınbaş University

Assoc. Prof. Dr. Aysel ERSOY

Department of Electrical and
Electronics Engineering,

Istanbul University - Cerrahpaşa

I hereby declare that this thesis meets all format and submission requirements of a Master's thesis.

Submission date of the thesis to Institute of Graduate Studies: ___/___/___

I hereby declare that all information/data presented in this graduation project has been obtained in full accordance with academic rules and ethical conduct. I also declare all unoriginal materials and conclusions have been cited in the text and all references mentioned in the Reference List have been cited in the text, and vice versa as required by the abovementioned rules and conduct.

Ali Riyadh Abdulmajeed AL-TEKREETI

Signature

DEDICATION

I dedicate this thesis to my family, classmate and all my friends for the support and encouragement throughout my education and life. Special dedication goes to my supervisor Asst. Prof. Dr. Mesut ÇEVİK, my father, my mother and my family for their support and prayers during my research work.



ACKNOWLEDGEMENTS

Please accept my sincere appreciation for all of the people who have stood with me throughout the duration of this journey. I'd want to give special thanks to my adviser, Asst. Prof. Dr. Mesut ÇEVİK, for being my compass even when I felt hopelessly lost and for being extraordinarily instrumental in shaping the final product of this study. I'd also want to express my gratitude to my boss, whose encouraging words contributed much to the success of this project. At long last, I want to thank this institution for being my home for the last few years. I owe a great debt of gratitude to my parents, whose beliefs and upbringing encourage me to always seek knowledge, to my siblings and extended family, whose affection I cherish beyond measure, and to my nation, which, while inanimate, grounds me and serves as an inspiration for perseverance.

ABSTRACT

LITHIUM ION BATTERY SOLAR CHARGER DESIGN AND SIMULATION

AL-TEKREETI, Ali Riyadh Abdulmajeed

M.Sc., Electrical and Computer Engineering, Altınbaş University

Supervisor: Asst. Prof. Dr. Mesut ÇEVİK

Date: 12/2022

Pages: 62

The charger work for lithium-ion batteries requires accuracy in performance, so charging must start at a voltage level commensurate with a constant current and the battery voltage to avoid the battery's temperature rising, which causes a reduction in its life. Exceeding the permissible limit will cause damage to the battery. In this work, a smart charger for a Li-Ion battery was designed and simulated. The proposed charger is supplied from the stand-alone PV array, and that is required to control both MPPT and battery charging at the same time. The charging sequence starts with constant current charging mode CC, when the SOC reaches a specific value then the charger changes charging mode into constant voltage CV mode. In CC mode, the PV array delivers its full power to the battery, but in CV mode, the PV array delivers a power equivalent to the battery charging capacity. The outcomes of simulations demonstrate that the system efficiency is near 95% in all studied cases. The proposed system can operate with the same efficiency even at variable irradiance levels.

Keywords: Lithium Ion, Constant Current, Constant Voltage, PV, MPPT, Smart Charger.

TABLE OF CONTENTS

	<u>Pages</u>
ABSTRACT	vii
LIST OF TABLES.....	x
LIST OF FIGURES.....	xi
ABBREVIATIONS.....	xiii
1. INTRODUCTION	1
1.1 OVERVIEW.....	1
1.2 BATTERIES BUILT FROM LITHIUM.....	2
1.3 THE PROBLEM OF TECHNICAL.....	3
1.4 SOLUTION OF PROBLEM	4
1.5 THESIS OUTLINE	5
2. LETERATURE REVIEW.....	6
2.1 PHOTOVOLTAIC PANELS MAXIMUM POWER POINT TRACKING TECHNIQUES	19
2.1.1 Indirectly MPPT	19
2.1.2 Abstract Criteria Direct MPPT.....	21
2.2 ALGORITHMS FOR CHARGING BATTERIES OF LITHIUM ION	21
2.2.1 Pulse Current	22
2.2.2 Multi-Stage of Current.....	24
2.2.3 Constant Voltage	24
2.2.4 Constant Current-Constant Voltage CC/CV.....	25

2.2.5	Variation of CC/CV Charging Strategies	27
3.	METHODOLOGY	33
3.1	SYSTEM COMPONENTS	33
3.1.1	PV Array.....	33
3.1.2	DC/DC Converter	35
3.1.3	MPPT And Control.....	35
3.1.4	Battery	39
3.2	OPERATION MODES.....	40
3.2.1	Constant Current Charging Mode.....	40
3.2.2	Constant Voltage Charging Mode	40
4.	SIMULATION RESULTS.....	41
4.1	CONSTANT IRRADIANCE CASE	41
4.1.1	System Performance In Case Of 1000 W/m ²	41
4.1.2	System Performance In Case Of 200 W/m ²	42
4.1.3	System Performance In Case Of 400 W/m ²	43
4.1.4	System Performance in Case Of 600 W/m ²	44
4.1.5	System Performance in Case Of 800 W/m ²	46
4.2	Variable Irradiance Operating Mode	47
5.	CONCLUSION AND FUTURE WORKS.....	49
5.1	CONCLUSIONS	49
5.2	FUTURE WORKS	49
	REFERENCES	50

LIST OF TABLES

	<u>Pages</u>
Table 3.1: PV array data	34
Table 3.2: Buck converter parameters	35
Table 3.3: Battery specifications	39



LIST OF FIGURES

	<u>Pages</u>
Figure 1.1: Block diagram of the control system	xiii
Figure 2.1: Schematic MPP for photovoltaic panel [8]	19
Figure 2.2: PV system with fraction open circuit voltage [10].....	21
Figure 2.3: Charging of lithium-ion batteries.	22
Figure 2.4: Pulse current charging.....	23
Figure 2.5: Characteristics of multi-stage current [11].....	24
Figure 2.6: CC/CV Profile [11]	26
Figure 2.7: Schematic representation of a double-loop control charge	27
Figure 2.8: Demonstrates the charging pattern of the BC-CC/CV	28
Figure 2.9: The charging patterns of the GP-CC/CV and the FL-CC/CV are demonstrated	29
Figure 2.10: Blocks diagram for PLL (CC/CV).....	30
Figure 2.11: Flowchart illustrating the process of charging the PLL- CC/CV.....	31
Figure 2.12: Displaying the charging pattern of the IPPL-CC/CV	32
Figure 3.1: Proposed system simulink model.....	33
Figure 3.2: PV array P-V & I-V curves.....	34
Figure 3.3: DC/DC buck converter simulink model.....	35
Figure 3.4: MPPT and control block	36
Figure 3.5: Nominal discharge current curves.....	40
Figure 4.1: PV and battery voltage and current curves	41
Figure 4.2: System efficiency	42
Figure 4.3: Battery and PV V&I curves in case of 200 W/m ²	42
Figure 4.4: P-V & I-V curves for the PV array in case of 200 W/m ²	43
Figure 4.5: System power and efficiency curves in case of 400 W/m ²	43
Figure 4.6: PV array P-V & I-V curves in case of 400 W/m ²	44
Figure 4.7: System voltage and current curves in case of 600 W/m ²	44
Figure 4.8: System power and efficiency curves in case of 600 W/m ²	45
Figure 4.9: PV array P-V & I-V curves in case of 600 W/m ²	45

Figure 4.11: System efficiency in case of 800 W/m²46
Figure 4.10: System voltage and power curves in case of 800 W/m²46
Figure 4.12: PV array P-V & I-V curves in case of 800 W/m²47
Figure 4.13: System voltage and power curves in case of variable irradiance47
Figure 4.14: System efficiency in case of variable irradiance48



ABBREVIATIONS

EVs	:	Electrical Vehicles
Li-ion	:	Lithium-Ion
CAGR	:	The Compound Annual Growth Rate
MPP	:	Maximum Power Point
MPPT	:	Maximum Power Point Tracking
MPC	:	Model Predictive Control
P&O	:	Perturb And Observe Method
CC	:	Constant Current
CV	:	Constant Voltage
CP	:	Constant Potential Voltage
SOC	:	State Of Charge
R-C	:	Resistor–Capacitor
OCV	:	The Open Circuit Voltage
ACKF	:	Adaptive Cubature Kalman Filter
DST	:	Dynamic Stress Test
NEDC	:	New European Driving Cycle
EKF	:	Extended Kalman Filter
CKF	:	Cubature Kalman Filter
HEV	:	Hybrid Electric Vehicle
TLBO	:	A Novel Teaching-Learning-Based Optimization

NMP : N-Methyl-2-Pyrrolidone
DWT : The Discrete Wavelet Transform
WNN : Wavelet Neural Network
L-M : Levenberg-Marquardt



1. INTRODUCTION

1.1 OVERVIEW

Every day more than gallons of gasoline are consumed worldwide. This level of fuel consumption has a devastating effect regarding the environment. If the fuel is burned, as is the case for the vast majority of it, as a result of the release of greenhouse emissions into the environment of the air, that are able to gather infrared sunlight from the sun (heat), the Earth's temperature rises; this phenomenon is known as global warming. As a result of producing CO_2 and H_2O , the petrol combustion reaction appears quite harmless and clean.; nevertheless, CO_2 and H_2O are the greatest contributions to the greenhouse effect, with H_2O being the most significant. In addition, the reactions in several automobiles and motors occur in confined compartments holding impure substances, leading in the development of more harmful byproducts as a result of the intense temperatures and pressures. Given that oxygen equals 21% of air and nitrogen 78%, the engine contains more nitrogen than oxygen. Due to the fact that there is more than twice as much nitrogen as oxygen, the extreme temperatures of petrol combustion mix these components to generate NO_x ., which is significantly more hazardous than CO_2 . Each of these greenhouse gases causes some degree of harm, but CO_2 is the most damaging. It will soon be necessary to make a substantial transition to sustainable energy sources such as wind, solar and hydro in order to abandon the use of gasoline. This energy should ideally be stored in a reusable medium, such as a battery. In the most recent decade of technical advancement, solar and battery technologies have advanced significantly. The necessity for environmentally safe technologies is the driving force behind the rise of the battery and solar industries. Due to the discovery of multi-level layer cells, solar cells with efficiencies of up to 44.7% are now commercially accessible and have been studied up to 24.1%. With these levels of efficiency. Now, renewable radiation has the potential to play a key part in electrical vehicles (EVs). The electrical vehicle's rechargeable battery is capable of storing energy for immediate or later use. Typically, a vehicle's battery is far larger than a house's battery, although the house might have a bigger solar system. Batteries are presently being doped with a variety of materials to optimize their properties for specific uses, including high power density for electric cars and high energy density for households. As an alternative to using coal or petrol to

power a home, solar panels and batteries can be installed on the roof; the exact same is true for automobiles. Utilizing clean energy for car is helpful, particularly if automobile cannot be readily linked into the power system but renewable radiation can indeed be. It has the capacity to store enough energy to go a predetermined distance, provide electric amusement, and regulate the temperature of the rechargeable batteries. Keeping both systems operational in close proximity to the identical voltage optimizes power transmission also decreases number of components necessary to convert between them. Due to the possibility that the devices would operate close to the same voltages, a buck-boost converter is required to transfer energy efficiently. Solar integration with electric vehicles is an innovative automotive component. Numerous production vehicles, such as the Fisker LeadAcid Battery, the Prius Fan, and a few others, have been outfitted with solar panels that power basic equipment. Nonetheless, the solar energy from an electric vehicle is capable of a lot more than just powering a blower or few onboard equipment, it may also the EV's rechargeable batteries, owing to present a high level of photovoltaic efficiency. It is substantially more beneficial to store electrical energy in the car's battery pack, as it enables the entire vehicle to operate. This is solar energy captured directly and kept for the owner's convenience for use right away. Sunlight is the best option for a source of energy. to electric vehicle due to linking to a grid that may contain tar energy is not a worry. The next stage in making solar more eco-friendly than gas is to create photovoltaic power from solar panels; therefore, the power must be saved.

1.2 BATTERIES BUILT FROM LITHIUM

The lithium-ion batteries utilization in battery-powered applications have expanded throughout time. The market for lithium-ion batteries is controlled by mobile computers, plug-in electric vehicles, and the military. This is owing to the high-power density, light weight and decrease self-discharge rate of these batteries. Lithium, although being the smallest metal, is exceedingly unstable and dangerous. It is necessary to mix it with other alloys in order to make it more stable and lessen the risks associated with using it and transporting it. Graphite is typically used the anode in lithium-ion batteries, while an oxide of a metallic behaves as the cathode and lithium salt use as electrolyte. The roles of cathode and anode are the two components of lithium-ion batteries switch according to if the battery is discharging or charging. The electrolyte the most

prevalent lithium-ion (Li-ion) and lithium ion polyethylene batteries is solid. The metal oxide cathodes of these two varieties may differ. Lithium manganese oxide, lithium titanate, lithium iron phosphate, lithium nickel oxide and lithium cobalt oxides are utilized as making cathode in batteries of Li-ion. The power density and nominal voltages according on the chemical composition. Batteries of Li-ion are offered in four simple shapes: cylinder shapes, both large and small, pouch shapes, and prismatic shapes [1]. Cylindrical shape groups are enclosed within a cylinder made of metal, whereas cylinder shapes are protected by a shell of rigid plastic. Pouch shape groups are stored in a soft foil bag, whereas prismatic shape groups are stored into semi-rigid plastic container. The Li-ion batteries benefits include their high power and energy density, the absence of a memory effect, a self-discharge low percentage, a relatively light weight. Despite its widespread use in a range of battery-powered applications, Li-ion batteries have significant limitations, including tight charging needs and deterioration caused by overcharging or severely discharging the battery. These are disadvantages vastly overshadowed by the numerous benefits, which is why it is employed in the great majority of battery-powered systems. According to TechNavio experts, the global lithium battery market would expand at a CAGR of 13.64 percent over the following three years [2]. According to Global Information Inc., the transportation industry's Li-ion battery revenue would expand from \$2 billion in 2011 to \$14.6 billion in 2017, the amount increased by 700%. This really is primarily due to plug-in hybrids and batteries electric automobiles [3]. This study will concentrate on filling some normal Li-ion batteries, as the Li-ion batteries are becoming increasingly popular option for producers of battery-powered products. The relationship between energy density and battery weight for various battery chemistries. The graph demonstrates that Li-ion batteries have a greater energy density at a reduced weight than alternative chemistries, culminating in ultimate market dominance.

1.3 THE PROBLEM OF TECHNICAL

As batteries and solar panels are significantly more powerful and vital than in the past, integrating them for power supply will be crucial in the twenty-first century. Li-ion batteries have vastly eclipsed utilization of lead-acid batteries and consequently greater significance to system under investigation. Due to these developments, the integration of solar panels and

batteries into electric cars is advantageous. This thesis addresses the technical difficulty of modeling regulator system for electric vehicle that is capable of transmitting the most amount of power from photovoltaic panels to battery without compromising the condition of the battery. Designing and modeling the operation of control systems allows for the identification of potential issues prior to their onboard testing. Consequently, more energy is taken in and put to use, and there is a corresponding decrease in the amount of energy that is squandered and emitted as pollution, as a result of the increased efficacy and total utilization of the power facilitated by specially built control systems.

To increase the quality of the system as a whole, the control system algorithm should be more analytical than other techniques already in use. The algorithm is resilient and never fails to continually track needed power point. Because the amount of sunlight that is absorbed by the screen is dependent on the angle at which the sun is shining, the voltage that is required in order for the panel to function properly varies when the EV has been driven; current to voltage curve of the solar panels differs, and the algorithm monitors MPP variation. In addition, lithium-ion batteries are charged during the process, but in a less straightforward manner than different chemical compositions of batteries. Chemistry related to batteries adds to complexity and process capabilities of control module since, in addition to MPPT, it must now assure proper battery charging.

1.4 SOLUTION OF PROBLEM

A representation of the block diagram for the control system as shown in figure below (Fig. 1.1). The use of a buck-boost converter, the duty cycle of which is governed by the control scheme, is depicted in the diagram as the method by which the solar panel transfers energy for the battery. To achieve maximum power point tracking efficiency, the control system measures the current and voltage on photovoltaic panel and adjusts the power converter's duty cycle (MPPT). The control system adjusts duty cycle in addition to giving the battery's current and voltage. The highest priority to stop battery from exceeding maximum ratings for both its voltage and its current. Construction the control system simulation and testing models is vital. The more effectively and accurately models are merged, the more potent the algorithm becomes. Simulink is used to construct the control algorithm due to its increased efficiency in system

modeling. Physical component models include the photovoltaic panels, battery, power electronics, and control algorithm. This significantly reduces the amount of mistakes associated with building a mathematical model of a complex circuit (containing switches) in MATLAB.

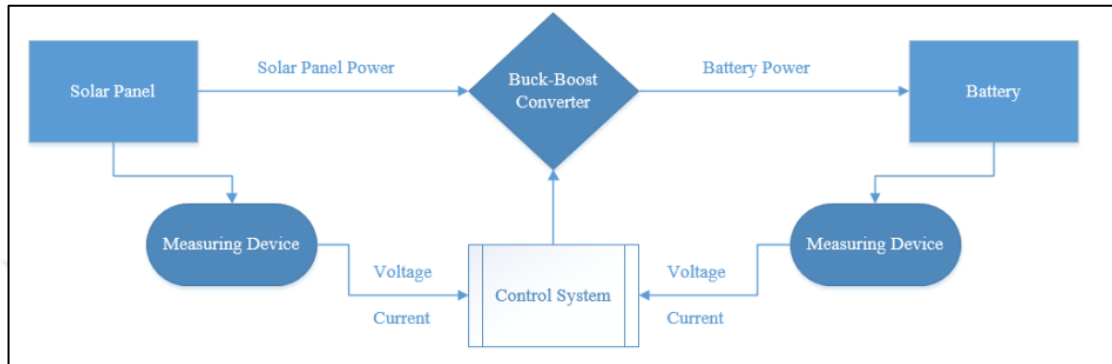


Figure 1.1: Block diagram of the control system.

This method of algorithm design can also be used to improve existing techniques; It saves time for test cases, stability can be validated before it is implemented, and all of the components may be customized.

1.5 THESIS OUTLINE

The literature review, the introduction, results, conclusion, simulation, future work make up remaining four chapters. In Chapter 2, we explore through Maximum Power Point Tracking (MPPT) for solar panels, the control systems research and techniques for related charge controllers, recharging techniques for lithium-ion batteries. The information that is presented in Chapter 3 is the foundational material needed to comprehend physical aspects for photovoltaic panels, the power converter and lithium battery. In Chapter 4, The control system is divided into schematic. The algorithm's formulas are then stated in parameter changes. The algorithm's parameters are then determined by case-by-case analysis. Finally, the algorithm is compared to other techniques that are already in use.

In Chapter 5, the management system is conclusively detailed, along with potential future modeling work.

2. LITERATURE REVIEW

In this part, studied, analyzed and knowledge about Li+ battery charging, MPPT and charge controllers with dual functionality is presented. This chapter is designed to be the key source of background information while maintaining the research's credibility. Energy savings, energy efficiency and replacement for fossil fuels instead of alternative renewable energy sources are three major technical advancements that are often incorporated in sustainable energy development programs. Renewable energy technologies have the ability to reduce global warming and greenhouse gas emissions by replacing renewable energy sources with traditional energy sources. The two primary types of solar energy are heat and light. The environment changes and absorbs sunlight and heat in a variety of ways. Improvements in the effectiveness of energy, solar PV manufacturing process, improved conversion efficiency and longer module lifetimes, have also garnered a lot of attention in order to decrease the energy payback period and reduce gas emissions. When opposed to certain other photovoltaic technologies, monocrystalline silicon consumes the most energy, the longest energy payback period, and the highest rate gas emissions. The high-level control in allows the rotational velocity of the DC motor to follow the required trajectory while simultaneously giving the necessary voltage profile for the DC/DC Buck converter's output voltage. The results demonstrate that requisite angular velocity is tracked accurately under the given conditions and even when the system parameters change unexpectedly. describes and categorizes MPPT techniques based on criteria such as the types of control strategies used and the types of circuits suited for PV systems, commercial and practical applications. For solar systems, employs a Model Predictive Control (MPC)-based MPPT algorithm. The results demonstrate that proposed control approach has good performance. A novel modified IC variable step size technique was established in. The experimental findings show good precision, faster convergence, and minimal oscillation⁴ around the MPP. As a result, the proposed IC algorithm is more efficient. A comparison of Buck versus Boost MPPT topologies is given in. A varying step size altered Perturb and observe method P&O algorithm has been devised, this may boost the PV system's dynamic and steady-state performance at the same time. The suggested variable step size solution solves problems in traditional methods. Different MPPT algorithms were investigated and simulated in under

varied irradiation circumstances. According to the simulation results, the P&O and Incremental conductance method IC algorithms have extremely similar performances and dynamic reaction times, and both systems have steady-state oscillation problems due to perturbations. In the convergence time MPPT performance of P&O and IC algorithms is compared. It is proved that the convergence time for IC is longer [4].

Photovoltaic system charging technologies are often highly confidential, and their operation methods are almost never revealed to the general. Substantial researcher has been undertaken on variety other combination architectures for solar panel battery charge. MPPT and effective battery charging must be combined in order to develop a solar array battery charger. On the market, there are numerous chargers with varied advantages for other purposes. Numerous solar array to lithium ion battery chargers have not yet been released; nonetheless, study on lead-acid batteries is readily available. The P&O MPP formula follows photovoltaics array. This is algorithm modified with pricing approach based on CC/CV. The algorithm uses CC/CV due to the maximum energy output of the panel may exceed the capacity of the battery. This setup, unlike the majority of chargers, uses lead-acid battery instead of a Lithium ion battery[5]. A hill-climbing algorithm for MPPT and a CP/CV charging method for Lithium-ion batteries. Their tracking approach is unique in that it uses hill-climbing algorithm rather than the P&O algorithm, which is standard for such controllers. However, their charging mechanism is the same as the standard method for such controllers[6]. By combining three separate lead-acid battery charging techniques with progressive conductance MPPT. Similarly, this system makes use of lead-acid batteries, which means that the techniques for charging them are different from those use for lithium-ion battery. To determine MPP, they rely only on incremental conductance, as opposed to a more effective hybrid technique [7]. Using a lead-acid battery, the P&O algorithm is investigated further. Despite the fact that they make no mention of any charging strategy, it may be deduced that they are focusing on MPPT. The algorithm's constant step sizes limit their capacity to perform MPPT [8]. Based on experimental test results, one kind model for the state of charge (SOC) lithium-ion battery is proposed here. The proposed model covers both the time progression and life cycle of SOC. Using Hill function characteristic, link between charge level and battery voltage is illustrated. The parameters of the model vary with the cycles

number and time dependent. Consequently, a modeling approach for SOC has been described and empirically validated. Initially, the two prevalent charging procedures, constant voltage (CV), constant current (CC), substantial differences between SOC and battery voltage were highlighted. The proposed model incorporates the Hill function, which provides greater shape flexibility while keeping an intelligible framework. It has been demonstrated that cycling a charge and the deterioration that this causes would have an effect on charging behavior. This effect can be precisely simulated with method that has been proposed by modifying the Hill parameters. Modifying the Hill order allows for the modeling of battery deterioration without the necessity for adding R-C pairs to analogous circuit. It has been demonstrated that the Hill function has advantages over polynomial fitting and the latter method needs estimate for coefficients larger number that is unrelated to deterioration. Because of how little computing it requires, the method that has been provided here is suitable for use in online SOC estimate models in battery operation simulation. In conclusion, the performance recommended model is based on a polynomial fit, the advantages of this modeling approach are discussed [9]. The deterioration of Li-ion battery cells is caused by a complex combination of several different chemical and physical processes. Li-ion batteries are also known as "lithium-ion" batteries. Loss of lithium inventory, lost effective positive electrode material, and lost effective negative electrode material are the three degradation modes that explain the observed physical impacts of these cell degradation mechanisms. The various mechanisms of deterioration are expected to have their own distinct and observable influence on open circuit voltage (OCV) of the Li-ion batteries and electrodes. As a result, diagnostic approach was tested for its ability to distinguish between six distinct types of degeneration. Only pseudo-OCV values are required for the diagnostic procedure after OCV model has been factorized. Because it takes pseudo-OCV measurements as input rather than the voltage or capacity derivative, it is less susceptible to noise than other methods that are stated in the literature. This is because it employs the OCV measurements. Because of these characteristics and the relatively low computational complexity of the diagnostic method, that is ideally suited for use in BMS applications to monitor the SoH of the cells and ensure that the operation is carried out in a risk-free manner. The diagnostic procedure that has been proposed is, in theory, applicable to all different types of Li-ion cell chemistries. This concept is going to get some further attention in forthcoming research. In

addition, a great amount of work is required to recognize and measure deterioration processes that occur in commercial Li-ion cells after they have been put through a wide variety of use scenarios and have been in operation for long length of time. Estimates of life span Li-ion batteries that are used commercial implementations should be provided as a result of this. To date, logical arguments rather than empirical data have supported the supposed nature and degree of these repercussions [10]. Temperature, for example, has an effect not just on OCV also capacity of the battery. Battery capacity tends to improve when temperatures are higher, whereas it tends to deteriorate when temperatures are lower. Consequently, including temperature as a factor in battery models improves battery performance. The impact that temperature has performance characteristics high-power Li-ion battery was evaluated with the help Li-ion battery that is sold commercially. The findings indicate that the principal impedances of li-ion battery are temperature dependent. In contrast, the battery model will also be influenced by the impact of aging. In fact, aging batteries can fail due to a reduction in capacity or an increase in internal resistance. The most prevalent type of battery equivalent circuit suffers from two distinct forms of deterioration: cycle deterioration, which is caused by storage period, and cycling deterioration, which is caused by frequent charge and discharge cycles. The models are going to be evaluated. These, when used as electrochemical models, generate partial differential equations with very large number of elements and variables unknown. Because of this complexity, there is typically a large Investigations into battery comparison models have been carried out specifically with the purpose of furthering the development of vehicle battery management systems and power management control. Several models have been developed and presented in the literature; however, the model that is most commonly used will be highlighted in this section [11].

The exact state of charge (SOC) evaluation lithium-ion battery is crucial for guaranteeing safe operation and preventing overcharging or over discharging. However, because SOC is an estimate, obtaining an accurate value is challenging.

A lithium battery's interior state, which cannot be physically examined. This paper describes an Adaptive Cubature Kalman filter-based SOC estimate algorithm for lithium-ion batteries in electric vehicles (ACKF). To obtain the battery model parameters, the lithium-ion battery is first

modeled using the second-order resistor-capacitor (RC) equivalent circuit and the memory factor least-squares approach. Following that, the Adaptive Cubature Kalman filter is introduced for forecasting remaining battery capacity, and the projected operation is demonstrated. The new method is compared to the standard extended Kalman filter (EKF) and cubature Kalman filter (CKF) algorithms using the Dynamic Stress Test (DST) and the New European Driving Cycle (NEDC). The findings of the studies show that the ACKF technique outperforms the standard EKF and CKF algorithms in terms of SOC estimate accuracy, convergence to various initial SOC errors, and robustness against voltage measurement noise. An Adaptive Cubature Kalman filter (ACKF) algorithm is developed to correctly estimate the SOC of lithium-ion batteries in electric vehicles. A similar circuit is used to replicate the nonlinear features of lithium-ion batteries and the creation of battery state-space formulae. For your convenience, a sixth equation has been inserted into the OCV-SOC connection, and the forgetting factor least-squares approach is used to derive the other RC parameters of the battery model. The theory of the adaptive cubature Kalman filter for estimating a battery's state of charge (SOC) is presented, as well as an approximated technique. Two popular driving cycles are used to test proposed performance: The Dynamic Stress Test and the New European Driving Cycle. Compared to the earlier EKF and CKF algorithms, the EKF and CKF algorithms, which are more recent. The results of the experiments demonstrate that proposed ACKF algorithm, despite fact that it requires more processing time than EKF and CKF, is beneficial for enhancing SOC estimate precision and integration to different starting SOC faults. This is the case despite the fact that the proposed algorithm requires more processing time than EKF and CKF. It also has a stronger ability to tolerate noise caused by voltage measurements than EKF and CKF [12]. A unified strategy for model-based real-time SOC.

This research looks at the capacity of lithium-ion batteries. To simulate the behavior of the battery terminals, an auto regression model is combined with a non-linear supplemental model to represent the hysteresis behavior. This is done to mimic the behavior of the battery terminals.

Off-line optimization of model parameters such as linear and nonlinear parameters is accomplished using a hybrid optimization approach that combines a metaheuristic method (also known as the teaching learning-based optimization method) with a genetic algorithm. This

strategy is utilized in hybrid optimization. The least squares method Second, two real-time model-based SOC estimate approaches are demonstrated using the trained model. One is based on the real-time battery OCV regression model obtained using the weighted recursive least square approach, while the other is based on condition monitoring using the extended Kalman filter method. The weighted recursive least square method was used to create both of these models (EKF). As a solution to the problem of flat OCV vs SOC segments that develop when using the OCV-based SOC estimation method, a method that combines coulombic counting with the OCV-based method is proposed. In the final stage, the simulation results and conclusions about SOC estimate are presented and evaluated using data from a LiFePo4 battery cell. Real-time accurate SOC estimation is crucial for the battery management system in EV/HEV applications. In this paper, both model-based estimate strategies and direct measurement techniques are presented for the purpose of calculating SOC. After that, an auto-regression model of the battery is constructed. A nonlinear supplementary model was constructed to incorporate battery hysteresis effect in order to simulate the behavior of the battery terminals. A hybrid technique that combines TLBO and the method of least squares is used, and it is applied to optimize model parameters. Two distinct models were produced by using the offline-trained model as their foundation.

We propose two real-time based SOC prediction approaches for Li-ion batteries: one is based on model parameter identification WRLS technique, other is based on state estimation EKF method. Both of these approaches are based on the assumption that the battery's state of charge can be accurately estimated. The joint-EKF approach is applied because the internal resistance of battery shifts depending on percentage of charge battery.

Use of for both parameter and state estimation was done so that performance SOC estimation could be improved. LiFePo4 battery cell's test results are used to compare and contrast the approaches that have been offered. There are two scenarios that are taken into consideration: one with an initial SOC estimation inaccuracy and one without. The findings of the estimation proved that the modeling strategy and model based SOC estimation methodologies, particularly joint-EKF technique, were correct.

It should be emphasized that the simulation and state-of-charge evaluation techniques mentioned in this work are data-driven techniques that employ onboard quantifiable terminal current and voltage readings. Additionally, these methods do not include any specific battery chemistries, which makes them generic for a wide range of applications. In this study, we look at the two challenges that are the most significant.

Evaluation SOC these different kinds of batteries can be challenging due to the straight OCV against SOC slope that exists over a variety of SOC ranges, as well as the hysteresis nonlinearity that exists throughout phases of charging and discharging. This study solely discusses the LiFePo₄ battery, the methods discussed here are applicable to a variety of other kinds of lithium batteries as good. NMP and LiCoO₂ batteries, in addition to cathode batteries, just one battery cell is explored in this particular study. Assuming that battery bundle is well balanced as a result battery management system, we can treat it as if it were a single massive battery cell and proceed accordingly. The subject of future research will be the process of calculating the SOC of a battery pack while the pack is in an imbalanced state. Furthermore, the temperature fluctuations of the battery system, which have an effect on battery behavior and, as a result, battery type identification, are not accounted for in this study. The impact of temperature on estimates of remaining battery capacity will be another area of focus for research in the future [13]. As the development on electric vehicles (EVs) continues, it is becoming increasingly important for accurately estimate state of charge (SOC). This is due to the fact that SOC is one of the most important factors for the battery management system., implying the amount of energy that is still available and helping to ensure that EVs are both safe and reliable. According to the findings this study, The SOC of lithium-ion batteries can be estimated using a hybrid wavelet neural network (WNN) model that combines the discrete wavelet transform (DWT) technique and an adaptable WNN. The Levenberg-Marquardt (L-M) method is used to prepare the WNN model, and discrete wavelet decomposition and reconstitution are used to process the model's inputs. In contrast to the process of back-propagation.

The proposed intelligent SOC includes back-propagation neural network (BPNN), L-M based BPNN (LMBPNN), L-M based WNN (LMWNN), and DWT with L-M based BPNN.

DWTLMBPNN with Kalman filter extension (discrete wavelet transform and Levenberg-Marquardt algorithm-based wavelet neural network) (EKF).

The estimate technique has been tested and confirmed to be successful. Under the New European Driving Cycle, the mean absolute error and maximum error can be reduced to 0.59% and 3.13%, correspondingly (NEDC). Based on comparative analysis and robustness assessment results, the suggested method's attributes of high accuracy and great robustness are proven by DWTLMWNN, a hybrid WNN model merging the DWT methodology and adaptive WNN, is presented to forecast the SOC of lithium-ion batteries (e.g., estimation error testing and inexperienced driving cycle test). The proposed intelligent SOC estimation approach has been validated and demonstrated to outperform BPNN, LMBPNN, LMWNN, DWTLMBPNN, and EKF. The features of great precision and strong robustness of the comparison analysis and robustness evaluation results validate the proposed strategy. It is discovered that the proposed analysis approach may address the BPNN- or WNN based techniques high max error problem (e.g., the max error of DWTLMWNN is reduced to 3.13% under the NEDC). There is considerable evaluation disturbance (e.g., 0.2 A/0.02 V arbitrary sounds) or the average absolute error and max error are kept at a reasonable level over untrained driving cycles. As a result, the suggested method is suitable and necessary for calculating SOC. [14]. In contrast to traditional multistage charging approaches, this research improves the transition among stages smoother and cuts down on the voltage drop that occurs within the cells' internal resistance when they are being charged. This is because the old Multiple Stage Charging Method used a single criterion, which said a stage shift happens as long as the voltage of one of the batteries surpasses 4.2 V. The reason for this is that this criterion states that a stage shift occurs. During the process of charging, the cell's internal resistance experiences a voltage drop, which causes the cell's voltage to rise above its actual value. This occurs because the cell's internal resistance approaches zero as the current approaches zero. When charging in the manner that is recommended, there is a steady reduction in this voltage drop, which results in a reduced amount of time spent charging. In addition to this, it is of the utmost importance to investigate the differences that exist in relation to the current situation between both the two cases. As a consequence of this, it is essential to take into account the fact that behavior proposed method varies depending on the

state of battery. Case 1, state of cells causes the cell voltage to drop significantly during the transition between current levels, this leads to increased internal resistance. This fall in battery voltage is caused by greater internal resistance. An adjustment to the existing level is required in order to bring the error down to a more manageable level. In scenario 2, the battery voltage lowers significantly less if there are no charge/discharge cycles.; as a result, the methodology that was proposed is similar to the typical multistage procedure. As a direct result of this, the suggested algorithm is able to react noticeably to the current state (number of charge/discharge cycles) of the batteries being recharged. The time required to charge anything is cut down by using the method described in this article for transitioning between different current levels. A new algorithm that combines charging and balancing is developed in order to improve the lifespan of large Li-ion battery packs. This is accomplished by combining the two processes. The system supports up to 168 series-connected cells due to its ability to control multiple battery packs under a single voltage limitation. We might, in theory, suggest this system to be unending power system because there are no restrictions on the number of cells that can operate in parallel with one another. This suggested algorithm beats the multistage technique since it demonstrates gentler changes in voltage while regulating current level. This ultimately results a shorter amount of time spent charging the battery. The benefit results from the fact that, unlike the normal method, instead of doing so automatically, the suggested solution regulates the present level using the difference among 4.2 V and the battery voltages. Notably, this method can adjust conditions used batteries. Regarding the duration of charging, voltage variation, and temperature increase, it was also possible to demonstrate that the proposed algorithm outperforms the standard multistage technique. After a battery of experiments, it was feasible to show that, with the BMS that is currently in use, top balancing is more effective than bottom balancing when it comes to balancing the current that is associated with the accepted profile. It is absolutely necessary for there to be connection between the charger and the BMS in order to make sure correct and safe charge [15]. There is a lack of uniformity that leads to a reduction in usable capacity, lifetime, and performance because to produce the appropriate voltage thresholds, many cells must be connected in series. In addition, there are both extrinsic and intrinsic differences between individual cells. In opposition to parallel cells, series-connected cells do not achieve self-balance [16].

This intrinsic (internal) non-homogeneity across cells is primarily caused by slight changes in the manufacturing process. These variances include differing capacities, volumes, internal impedance, and self-discharge rates, all of which degrade with usage and as the battery ages. Temperature heterogeneity across the battery pack is the most critical extrinsic element because it generates varying self-discharge rates and, as a result, performance declines [17]. Several methods of battery balancing that have been described in research writings to develop a system that can execute a charging algorithm. The most often utilized balancing system serves as the foundation for the dissipative resistors technique [18]. This technique was chosen for this study because of its ease of use, affordability, efficiency, volume, weight, durability, and dependability. Lithium-ion batteries typically have an operational voltage range that falls somewhere between 3 V and 4.2 V. A deep state of discharge could occur if the voltage falls below the lower limit, which will ultimately result in the death of the cell. In addition, if the voltage is greater than 4.2 volts, the cell may be damaged due to an increase in temperature [1]. Therefore, understanding each cell's voltage and taking safeguards are crucial to preventing severe damage. [19]. In this paper, battery management system (BMS) is discussed that is capable of monitoring an energy storage that is potentially unlimited. Because it needs information the voltages each individual cell and pack, balancing and charging the batteries necessitates the use this monitoring system. In addition, the acquisition unit is able to detect the state of the battery, which includes the identification of static defects, as well as the max and min cell voltages and temperature. The voltage rechargeable battery, which consisting of 168 series connected cells is the one thing that prevents this method from being completely effective.

There are numerous approaches to charging batteries that may be found in the research that has been done, but very few of them are suitable for charging large Li-ion battery packs. Therefore, it is of the utmost importance to monitor and manage the voltage of each and every one of the cells, as failure to do so may result in the voltage of the cell reaching levels that are fatal [20]. This study proposes an algorithm that is based on the multistage method and it integrates charging and balancing techniques into a single process. The criterion that will be used to transition between existing levels is one of the more intriguing modifications that has been offered. This transition can be determined by computing the difference between the actual

voltage of the cell and the voltage that is desired. The method that was created also takes into account the charging current, which enables an estimation of the charge's condition to be made. It is essential for large Li-ion battery packs to have cell equalization, which is made possible by the inclusion of a balancing mechanism in the algorithm [15]. This is another significant component of the algorithm. As the charging process continued for a longer period of time, the battery voltage gradually grew to roughly 4.25 volts, but the temperature of the battery initially dropped from 35 degrees Celsius before rising again. Insufficient time had passed to ensure that the battery's internal chemical reaction had established a suitably stable state, which led to a drop in temperature during the initial charging phase of the process. This was a result of the decrease in temperature. There is a general coherence between the voltage and temperature profiles of the three best charging techniques that have been detailed. The three-stage charge at constant current took the least amount of time, with the battery reaching full capacity at 6870 seconds after completion of the charging process. The four-stage charging with constant current took the longest to complete, requiring a total of 7 998 seconds. In addition, the total time required to charge the battery using a constant current and five stages was 7339 seconds. However, the temperature spike that occurred during the three-stage constant current charging was the most noticeable. There was a difference of approximately 2 degrees Celsius between the peak and lowest temperatures of the two battery samples throughout the charging procedure. A comparison of the current, voltage, and temperature curves of the two different battery samples while they were being charged using either the optimal charging strategy or the 0.5C CC-CV charging strategy. The amount of time that was needed to charge the two battery samples using the 0.5C CC-CV method was 8551 s and 8490 s, respectively, but the four-stage optimized charging strategy that required the most amount of time had an average time reduction of 6.13% when compared to the 0.5C CC-CV charging strategy. The highest temperatures that could be achieved during 0.5C CC-CV charging were 34.61 and 34.52 degrees Celsius. These temperatures were 1.65 and 1.62 degrees Celsius higher than the temperatures that were achieved at their lowest, which were 32.96 and 32.9 degrees Celsius. Not only did the proposed technique of charging with five stages of constant current have a maximum temperature that was 34.28 degrees Celsius lower than the 0.5C CC-CV charging method, but it also decreased the amount of time it took to charge by an average of 13.87 percent. The five-stage constant

current charging method that was reported in this study appears to be advantageous as a result of the reduction in charging time as well as the rise in temperature. Therefore, a method for optimizing lithium-ion battery charging based on an enhanced electro-thermal coupling model is designed to address the issue of existing lithium-ion battery rapid charging as well as the visible temperature rise that occurs throughout the charging process. The dynamic performance of the battery was simulated by constructing a model of a second-order RC equivalent circuit, and the parameters of the battery model were determined by employing the least squares approach. During the process of developing the thermal model of the lithium-ion battery, an electric-thermal coupling model was also established. For three-stage, four-stage, and five-stage constant current charging, respectively, the particle swarm algorithm was utilized to determine the optimal charging current curve and provide the least value of the goal function, which included charging time and temperature rise. This was done for each stage individually. The trials that were done to validate the system employed the exact same model and batch of batteries because that is the charging method that yields the best results. The findings of the experiments suggest that, in contrast to the 0.5C CC-CV charging mode, the optimized multi-stage constant current charging technique that was proposed may be able to successfully address the issue of the temperature of the battery skyrocketing dramatically during the charging process as a direct result of the use of fast charging. The five-stage constant current charging approach reduces peak temperature by 0.83 percent in contrast to the 0.5C CC-CV charging method, and it reduces charging time by 13.87 percent on average. Future adjustments and improvements to the optimal charging technique can take into account issues such as battery aging and life loss [21]. In order to overcome power quality issues in power systems, a new controller based on the synchronous reference frame (SRF) is proposed for a photovoltaic (PV) panel supported three-phase universal power quality conditioner (PV-UPQC). In the PV-UPQC system, serial and parallel active power filters are fed by PV panels. The proposed controller collects measurement results from four distinct locations across the power system. The reference current and voltage values are derived based on the measured values and the DC voltage produced by PV panels. Moving average filters and space vector-PWM are utilized to produce PWM signals for active filter switches. The algorithm applied in both filters is separated into two components. The first

algorithm MPPT, derives the maximum voltage from the PV panels, while the second, SRF-based proposed technique, obtains the reference current or voltage.

Simulation and experimental tests are performed on the suggested controller. In terms of harmonic current and voltage attenuation, the recommended controller for three-phase PV-UPQC exceeds the standard SRF-based controller [22]. The proposed system consists of series and shunt inverters coupled through a dc-link to a photovoltaic array. By injecting active power into the grid, this system can adjust for voltage and current issues in both interconnected and islanding modes. The primary problem is that sensitive equipment (SE) and power electronic devices (PE) are often built to function properly in power systems that are not polluted, and as a result, they will malfunction if the supply voltage is not pure sinusoidal. Integrating photovoltaic arrays with centralization of power quality conditioners is one way that the proposed guidance with variable operation mode might enhance the power quality of the grid system. All three-phase, four-leg inverters utilize a technique known as pulse width modulation, or PWM for short. The quality of the electricity is improved with the use of Proportional Integral (PI) and Fuzzy Logic Controllers, which both work to reduce the amount of distortion in the power output. A description of the results that came from a study that compared the performance of paired Unified Power Quality Conditioners and photovoltaic systems. In order to compensate for swell, interruption, reactive power, voltage drop and harmonics in both islanding and interconnected modes, the system is made up of series and shunt inverters, a PV module, and a DC/DC converter. The cost of connecting the PV interface inverter to the grid can be reduced by using a UPQC shunt inverter, and compensating for voltage disturbances can be achieved by connecting the PV array to a DC connection. The P&O approach is going to be used in this suggested system in order to determine the PV array's maximum power point. A fuzzy controller is superior to a PI controller due to the fuzzy controller's faster reaction time and more thorough rectification of erroneous voltage from the source. Fuzzy logic is significantly simpler to use when a fault happens at the supplier, occupies less space to enforce, and, most importantly, is markedly more cost-effective than PI controller. This is because fuzzy logic regulates itself during the type of failure that is obtained in the source voltage [23].

2.1 PHOTOVOLTAIC PANELS MAXIMUM POWER POINT TRACKING TECHNIQUES

MPPT is significant technique for optimizing the amount of energy harvested via solar irradiance. The maximum power point (MPP) of a photovoltaic panel is its area with the highest electrical efficiency, as shown in figure below (Fig. 2.1). Numerous systems exist on the market for MPP tracking of photovoltaic panels, but only a few have been thoroughly studied as controls: Hill-climbing, constant voltage, partial open circuit voltage, P&O, progressive neural networks, fuzzy logic, voltage/current sweep, and conductance. On the basis of their level of complexity and the approach they employ, each of these methods can be grouped into one of three categories: those that are immediately powered by physically criteria, those that directly utilize physical criteria, and those that directly depend on abstraction criteria.

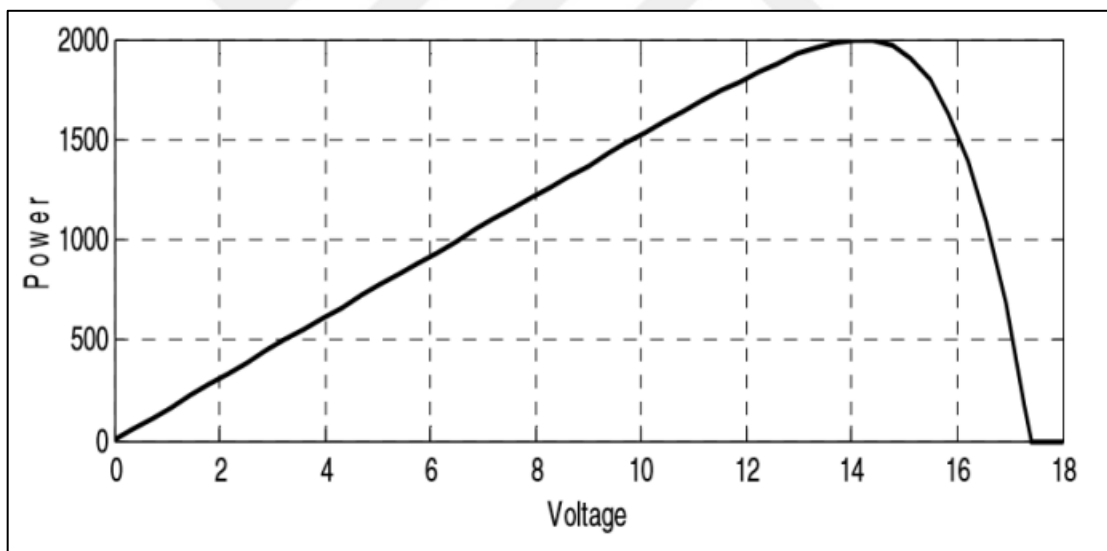


Figure 2.1: Schematic MPP for photovoltaic panel [8]

2.1.1 Indirectly MPPT

The indirect MPPT techniques are pre-optimized for photovoltaic panel's features and anticipated ambient circumstances, and they don't require measuring instruments.

The fixed voltage control method aims to keep the solar panel's optimal voltage constant under all circumstances. The MPP of the solar panel doesn't vary much based on voltage under a variety of weather and temperature circumstances, which is why it has been employed. its

surroundings. Of all the MPPT methods, the fixed voltage control technique has the fewest steps to follow but suffers the most difficulties in monitoring the MPP. It maintains the photovoltaic panels at a fixed voltage, though often not at the MPP because the P-V curve of photovoltaic panels are continually shifting in response to the environment. Because the constant voltage had been set to that specific condition on first day, this method might function perfectly. However, if clouds occur, The MPP has altered as the photovoltaic panels matures or the temperature fluctuates; hence, the method may now be inefficient or perhaps worthless. This approach has the benefits of being easy to apply, requiring no measurement instruments, converges to the optimal MPP voltage very quickly, and being the most stable under any circumstance. The drawbacks include the fact that it isn't actually tracking MPP, that it might be utterly worthless, and that it frequently needs to be re-optimized or adjusted for new voltage levels [24].

The fraction open circuit voltage control method computes the photovoltaic panel's voltage maintenance depending on an optimum real number of the comparative voltage of the open circuit in relation to any particular circumstance. This indicates that the algorithm detects for open circuit voltage and factors it by real number in order to establish the voltage at which the solar cell should be maintained. Extensive study has found that there exists a fraction scaling factor quantity that produces a voltage close to MPP, hence this method is effective. As illustrated in figure below (Fig. 2.2), When the P-V curve shifts because of changes in irradiance or temperature, the open circuit voltage shifts along with it, and the MPP voltage is almost always the precise proportion of the open circuit voltage. The partial open circuit voltage control approach is marginally more complicated than the constant voltage technique, but it provides a substantially greater improvement in picking a voltage that is nearer to MPP. This method has a number of benefits, including as rapid converging rates to an optimal parametric voltage, the absence of monitoring equipment, and simplicity of implementation. Therefore, the MPP does not follow and it requires continual re-optimization or tweaks to the scalar value. Additionally, it must constantly reevaluate the voltage in the open circuit [25].

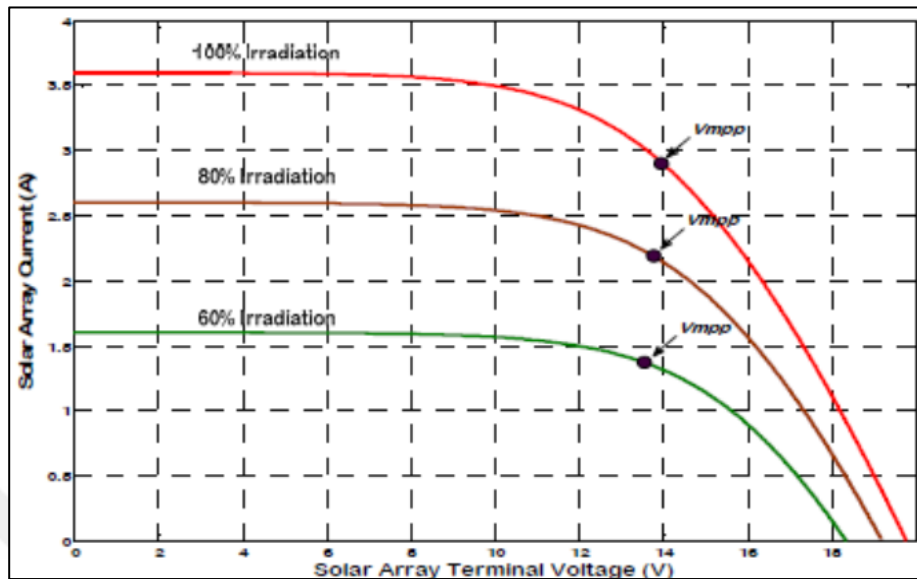


Figure 2.2: PV system with fraction open circuit voltage. [10]

2.1.2 Abstract Criteria Direct MPPT

To decide next action, the abstract-direct MPPT approaches, like physical-direct MPPT, involve sensing the current and voltage. These techniques are abstract concepts directly since in spite of the fact that they are calibrated for specific settings in the same way that indirect MPPT techniques are, they are constructed on abstract notions that allow them to perform MPPT faultlessly and without some of the faults that are inherent to physical-direct approaches.

2.2 ALGORITHMS FOR CHARGING BATTERIES OF LITHIUM ION

During in the discharging (charging) operation, In this method, lithium ions are momentarily injected into or derived from two porous electrodes that are submerged in a fluid electrolyte that contains the charged species Li^+ ions [26]. The foil that separates the electrodes also prevents electrical contact between them. In some lithium-ion batteries, the solid electrolyte doubles up as both an ionic conductive medium and an electrical insulator separator. This allows the battery to perform two functions at once. These batteries can also be referred to as lithium polymer or lithium battery polymer cells. Lithium-ion batteries are the most common type. However, regardless of whether the electrolyte in the cell is liquid or solid, the charged species that intercalate within the cell are Li^+ ions; as a result, these batteries are sometimes referred to as lithium-ion batteries. The process of inserting or extracting lithium, which requires an ion flow

through the electrolyte, is accompanied by the reduction (oxid) reaction of two electrodes, which is helped along by an ion transport through the external circuit. This reaction takes place simultaneously. As shown in figure below (Fig. 2.3), which is a diagrammatic representation of a lithium-ion battery being charged, Li^+ ions are extracted from the top anode of the battery and injected into the electrode that has a negative charge. This process is known as cathode charging. The amount of energy that can be stored in lithium-ion batteries after they have been charged is determined by the difference in the energy levels of the interpenetrating Li^+ ions that are found in the positive and negative electrodes [27],[28],[29]. There are a few different approaches to charging lithium-ion batteries, but the constant current to constant voltage (CC/CV) method is the one that is generally acknowledged as being the most dependable and widely used. The constant voltage charging method, the multi-stage current charging method, and the pulse current recharging method are a few more. Depending on the charging system, each of these solutions has a unique set of benefits and drawbacks to provide as compared to the CC/CV approach.

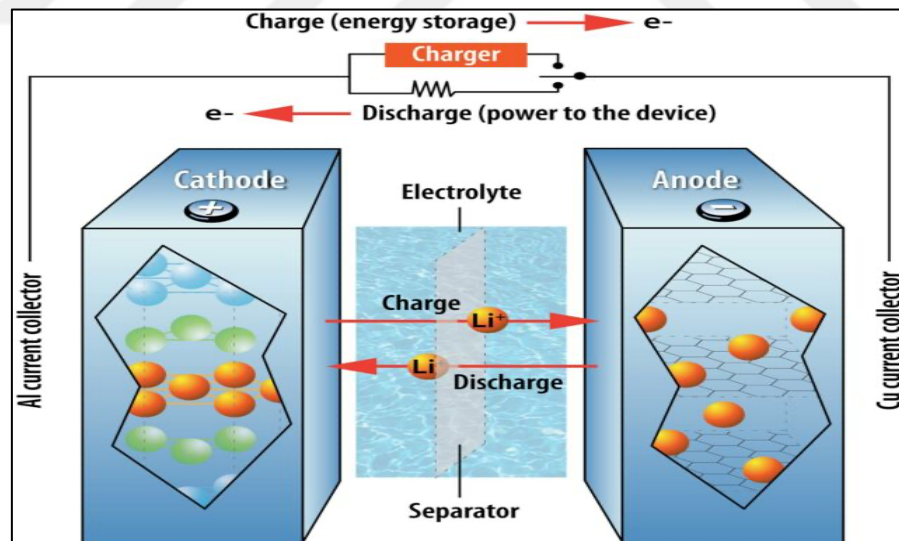


Figure 2.3: Charging of lithium-ion batteries. [27]

2.2.1 Pulse Current

As shown in figure below (Fig. 2.4), pulse current charging involves sending current pulses to the batteries at a level of current that has been predetermined, and as the battery gets closer to being fully charged, the duration of the pulses gets shorter. This method of preventing the battery

from being overcharged while it is being recharged is straightforward yet adaptable. Even when charging systems are only capable of producing a single rate of current output, it is still possible for them to replenish the battery; however, they must be able to adjust the pulse length. Although this technique is employable, the technique has potential to lead to the battery for reaching its maximum voltage near the conclusion of its charging process, potentially causing the battery to be damaged and the electrochemical reaction to be ruined due to over-polarization. This charging method is advantageous due to its simplicity and ability to fully charge a battery with a single current. Negative aspects include pulse widths that must be modified dependent on the comparative battery voltage and the inability to keep a consistent battery voltage at the end of charge [30], [31]. It has been discovered that pulse charging improves batteries charging and energy efficiency while also reducing charge time [32],[33],[34]. It also increases safety because the relaxation intervals between charging current pulses for Li^+ to intercalate successfully and help prevent dendrite development [35]. Identifying and defining the variables that result in the most effective battery performance is challenging when designing and implementing pulse charging algorithms. The battery output performance measures, such as battery charging and energy efficiency, cycle of life, and low duration, will vary depending on the selection of these characteristics and their levels. While pulse charging has been discovered to be more effective, the effect of these elements and their degrees on the charge / discharge of the batteries and its resistance parameters is hardly investigated.

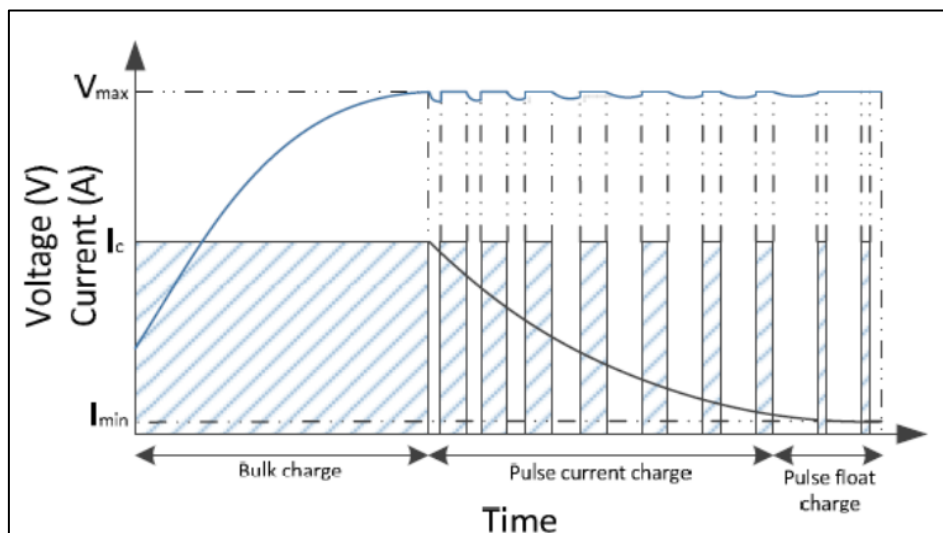


Figure 2.4: Pulse Current Charging.

2.2.2 Multi-Stage of Current

As depicted in figure below (Fig. 2.5), multi-stage current recharging allows the charging system to charge at multiple stages. Whenever the cell has reached its maximum voltage after being charged at a constant rate for an extended period of time and has reached its maximum capacity, a next reduced current stage is applied until the battery again reaches its maximum voltage, and the process is continued until the most basic level is accomplished. This is technique for recharging the battery is technically healthier than pulsed charging because it does not surpass the maximum voltage and instead gradually increases the current. This method has the advantages of being easy to install, recharging batteries securely, and functioning with separate charging systems. This charging method has the drawbacks of not being able to swiftly bring the batteries up to maximum voltage and not being able to maintain the battery at higher voltages throughout the final charging period [31].

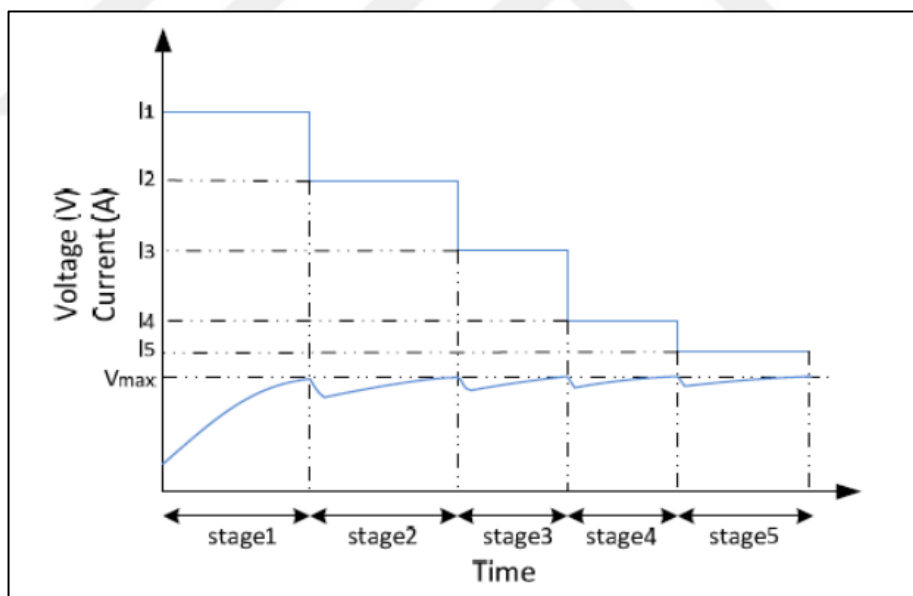


Figure 2.5: Characteristics of Multi-Stage Current [11].

2.2.3 Constant Voltage

The voltage of fixed recharging keeps the voltage from through battery based on the charging pace. This voltage is occasionally greater than the battery's ideal value in order to speed up the charging process; however, this can push a great deal of potentially and current degrade the

battery's properties. Battery should be charged to its peak voltage if the current does not induce heat reactions that degrade the battery's electrochemical features. By using various steps, the voltages of constant to sustain the battery decrease likelihood of battery degradation, because of charge times are frequently lengthened., which this because is larger voltage levels are commonly employed across the battery. When the battery's charge is nearly depleted, the best battery voltage is supplied across the cell to obtain it while preventing overcharging. This system's advantages include its simple use, rapid charging, and flexible settings. The disadvantages of using this charging method include the fact that it is unable to charge the battery under the current conditions and that it poses a danger of harm while being recharged and the fluctuating energy density onto the battery [31].

2.2.4 Constant Current-Constant Voltage CC/CV

As CC/CV charged the batteries at a constant current, followed by a constant voltage. This technique of the battery's charging is the most durable and safest since it does not place an excessive amount of current through the batteries or an excessive amount of voltage through the terminals. The completion of the charging process with constant voltage can take an extremely long time if that voltage is where the battery wants to be charged to; this problem can be fixed by slightly continuing to increase the constant voltage value so that more current is inputted; however, doing so can again be harmful to the battery. This technique can be extremely slow than other approaches because of this. In contrast to the other three charging methods, this charging approach offers controlled charging systems and necessitates the use of equipment that is capable of recharging at a constant current and voltage. Because of its simplicity and ease of implementation, the constant current constant voltage (CC/CV) charging method for lithium-ion batteries is extensively researched and widely utilized. The CC/CV charge algorithms charges the batteries with a constant current until the battery voltage reaches a predetermined maximum charging voltage (V_{preset}), Until this point, the charging voltage has been kept constant while the charging current has been steadily decreasing. When the charged current reaches a minimum value that has been predetermined, the procedure for charging the battery is complete. as shown in figure below (Fig. 2.6), presents the CC/CV charging profile for your reference. Utilizing the CC/CV to generate a charger for a lithium-ion battery necessitates the

implementation of a variety of preventative measures to ensure the integrity of the battery. The charging procedure of a charger is depicted in Figure 3, which is based on the CC/CV. When charging in CC mode, the total charging time can range anywhere from one to two and a half hours depending on the charging current. In general, the charging current in CC mode should be kept as low as possible. This will result in a higher charging efficiency, a longer charging time, and an increased battery life. Typically, three sensors are required in order to accurately measure the voltage, current, and temperature increases of a battery. Because it does not require a microcontroller, the CC/CV charging algorithm can be easily and affordably implemented with little effort. The capacity of this technology to charge a battery at a steady pace up to 80% faster, the utilization of safe energy on a battery, and the technology's endurance are the advantages that come with its use. A number of negative elements include the difficulty in fast charging the battery at the conclusion of the charge cycle, the presence of a high number of input and output devices, and an increase in battery power when the charge cycle is in its constant current phase. When the battery is able to resist the maximum power output of the charging equipment, the CP/CV charging method is a viable option to using this method [30],[31].

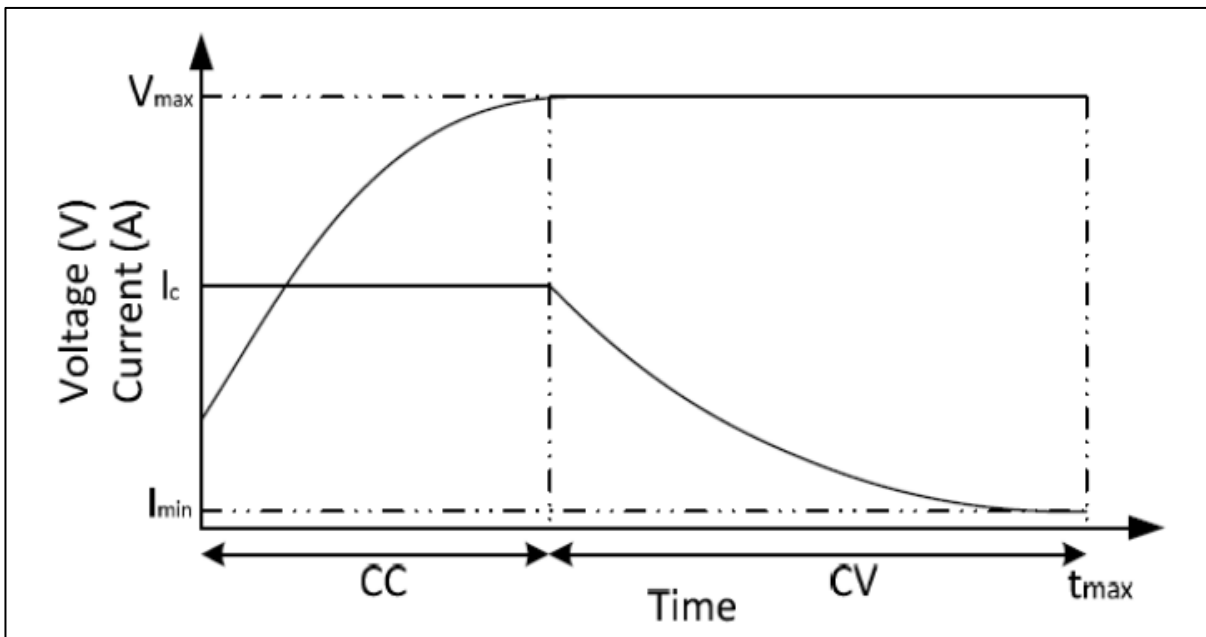


Figure 2.6: CC/CV Profile [11].

2.2.5 Variation of CC/CV Charging Strategies

There have been many different iterations of the CC/CV recharging optimization algorithm. Two of these were produced as a result of a change made to the standard CC/CV charging procedure. In (Fig. 2.7) provides an illustration of an example of the double control charge (DL-CC/CV). Utilizing both positive and negative feedback on the voltage of the battery ($V_B(s)$). Consequently, there is no longer a requirement for a current sensor, but similar CC/CV performance is maintained utilizing the simplest and cheapest hardware approach.

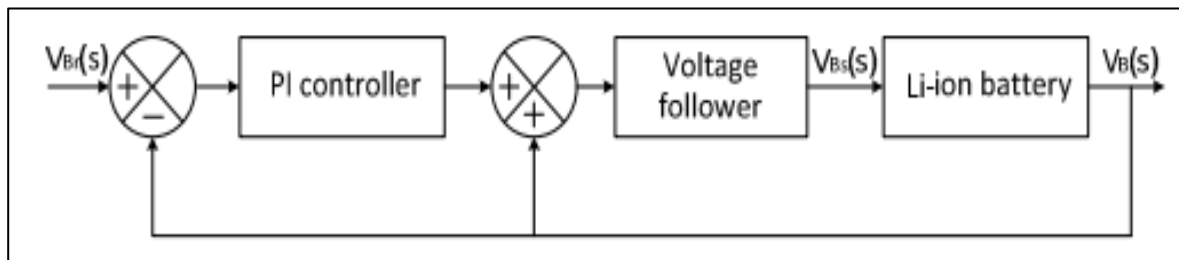


Figure 2.7: Schematic representation of a double-loop control charge [19].

The second kind of charger is called a boost charger (BC-CC/CV) [20], and it calls for the battery to be completely drained before it can begin charging. For charging purposes, the BC-CC/CV makes use of the CV charging method at the peak power V_b^{\max} (for example, 4.3V, which is greater by 0.1V than 4.2V) to keep the battery charged during the period designated for boost charging t_b (for example, 5 minutes), and the capacity after charging can reach approximately thirty percent of its maximum capacity. This demonstrates that the battery was able to store a significant amount of charge in a very short length of time t_b . It is possible to charge the battery to approximately sixty percent of its maximum capacity if this time period is increased to ten minutes.

After this period of time has passed, the charge methodology will go back to the standard CC/CV. As shown in figure below (Fig. 2.8), presents a visual representation of the charging pattern of the BCCC/CV. As a result of the higher starting charge voltage, the BCCC/CV has the potential to charge the battery more quickly than the CC/CV does; nevertheless, the battery needs to be completely drained before it can be charged, which requires the utilization of a discharging circuit. Both the number of parts and the overall cost will rise as a result of this.

Because it first requires draining the battery, this charging approach is not only ineffective but also wasteful. The impact that an increased initial charging voltage has on the lifespan of a battery has been investigated. After five hundred iterations of testing, there is no obvious drop in quality.

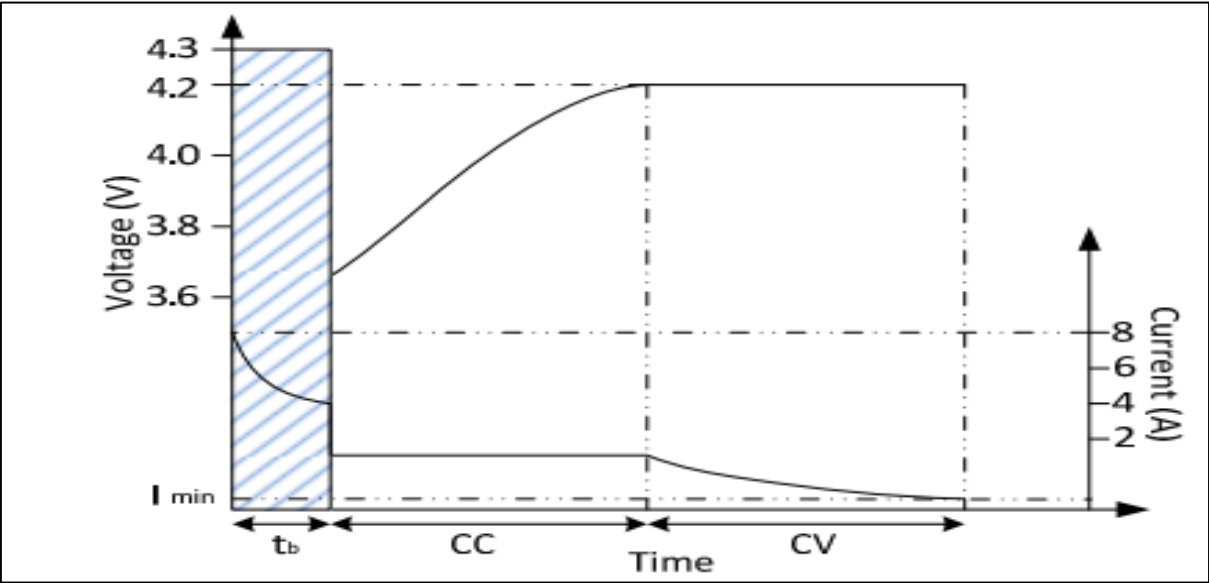


Figure 2.8: Demonstrates the charging pattern of the BC-CC/CV.

There are two more algorithms that can also achieve CC/CV, and both of them make use of sophisticated control. The grey-predicted control and the fuzzy-logic control were utilized in these two charging algorithms, which are referred to as the FL-CC/CV [37] and the GP-CC/CV [38], respectively, in order to maximize the charging current while operating in the CV mode of the CC/CV. These two charging algorithms are referred to as the FL-CC/CV [37] and the GP-CC/CV [38]. FL-CC/CV and GP-CC/CV are the names given to these two different charging algorithms, respectively. In each of these charging algorithms, the voltage at the open circuit is the one that is employed as the changeover voltage when transitioning from the CC mode to the CV mode. This makes certain that the charging current of the CV mode of the regular CC/CV charging algorithm is greater at higher current parts and lower at reduced current parts than the charging current in the CV mode of the CV mode of the normal charging algorithm. A consequence of this, additional capacity can be loaded into the battery in the same amount of time as was required by the CV mode. The charging profiles for both methods are represented

pictorially in figure below (Fig. 2.9), which may be seen here. In order to dynamically determine the appropriate charging current while keeping an OCV of 4.2V in CV mode, a fuzzy-controlled active state of charge controller has been used for the FL-CC/CV and a grey-predicted technique has been used for the GPCC/CV. Both of these controllers have been used in the CC/CV systems. The FL-CC/CV and the GP-CC/CV have a shorter length of time necessary for charging and a greater charging efficiency as a direct consequence of this. Additionally, the charging process takes less time. Because of the complexity of each of these charging methods and the significant amount of processing power that is required, the microcontroller presents the best opportunity to put these algorithms into action. Another approach to charging is based on the principle of phase-locked loop (PLL) regulation [39], which serves as the method's foundation.

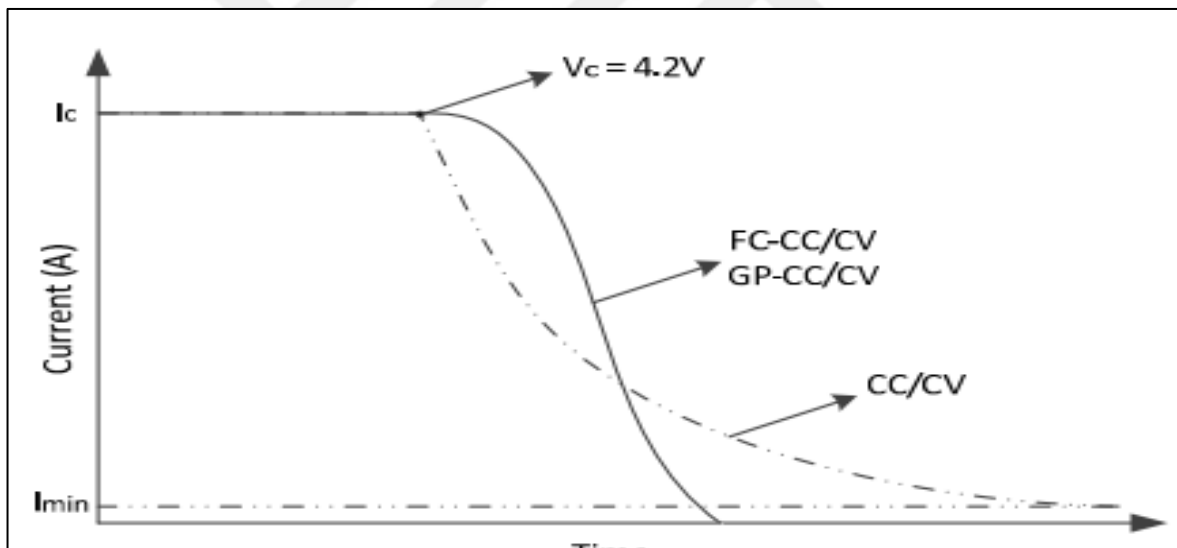


Figure 2.9: The charging patterns of the GP-CC/CV and the FL-CC/CV are demonstrated [39].

The PLL procedure naturally correlates with the CC/CV charging profile need (PLL-CC/CV). The PLL-CC/CV block diagram is shown in figure below (Fig. 2.10). According to Fig. 2.10, the VCO output demonstrates an oscillating feedback wave P_o , it has repercussions for the voltage of the battery V_b . The phase error P_e is then calculated by comparing P_o to the input reference phase P_i . This phase error P_e is delivered to the current pump, this produces the correct amount of current for lithium-ion batteries to be charged. After a certain number of cycles, the battery will be able to accept a complete charge.

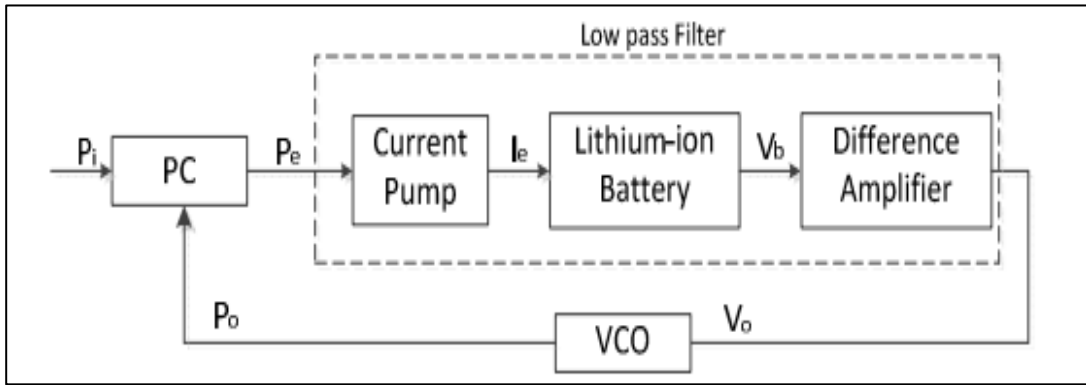


Figure 2.10: Blocks diagram for PLL (CC/CV).

This PLL-CC/CV configuration's bulk charge corresponds to the auto-tracking process, which is the same as the CC mode of the CC/CV. The CV mode of the CC/CV is the same as well. This is the case due to the fact that the frequency-tracking procedure is the same for both modes. The auto-locking process, which transitions from phase-tracking to a phase-locked state, is comparable to the variable current charge and float charge modes of the CC/CV. Phase-tracking is the process in which a phase signal is tracked in order to determine the next phase of the signal. When the process of automatically locking the device is finished, this mode is enabled. The process of charging the PLL-CC/CV is illustrated in the figure labeled (Fig. 2.11), which can be seen below. Later on, an improved PLL-CC/CV known as the IPLLL-CC/CV was made available to the general public [40]. The entire process of charging consists of the bulk current charge (CC mode), which continues to be the same as that of the PLL-CC/CV, as well as the pulsed current charge and pulsed float charge (CV mode), both of which were modified from the varying current charge and the float charge, respectively, as shown in (Fig. 2.12). The bulk current charge is the only part of the charging process that has not changed. The PLL-CC/CV mode continues to operate in the same manner as the PLL-CC/CV mode. The efficiency with which the upgraded IPLLL-CC/CV charges is superior to that of the standard CC/CV. This is because the internal pressure that is charged by a pulsed current is smaller than that which is charged by a constant current. This is because a constant current charges at a more consistent rate. It takes roughly the same length of time as the CC/CV for the battery to completely charge. Using an integrated circuit device that has a PLL function makes it possible to construct both the PLLCC/CV and the IPLLL-CC/CV in a simple and straightforward manner.

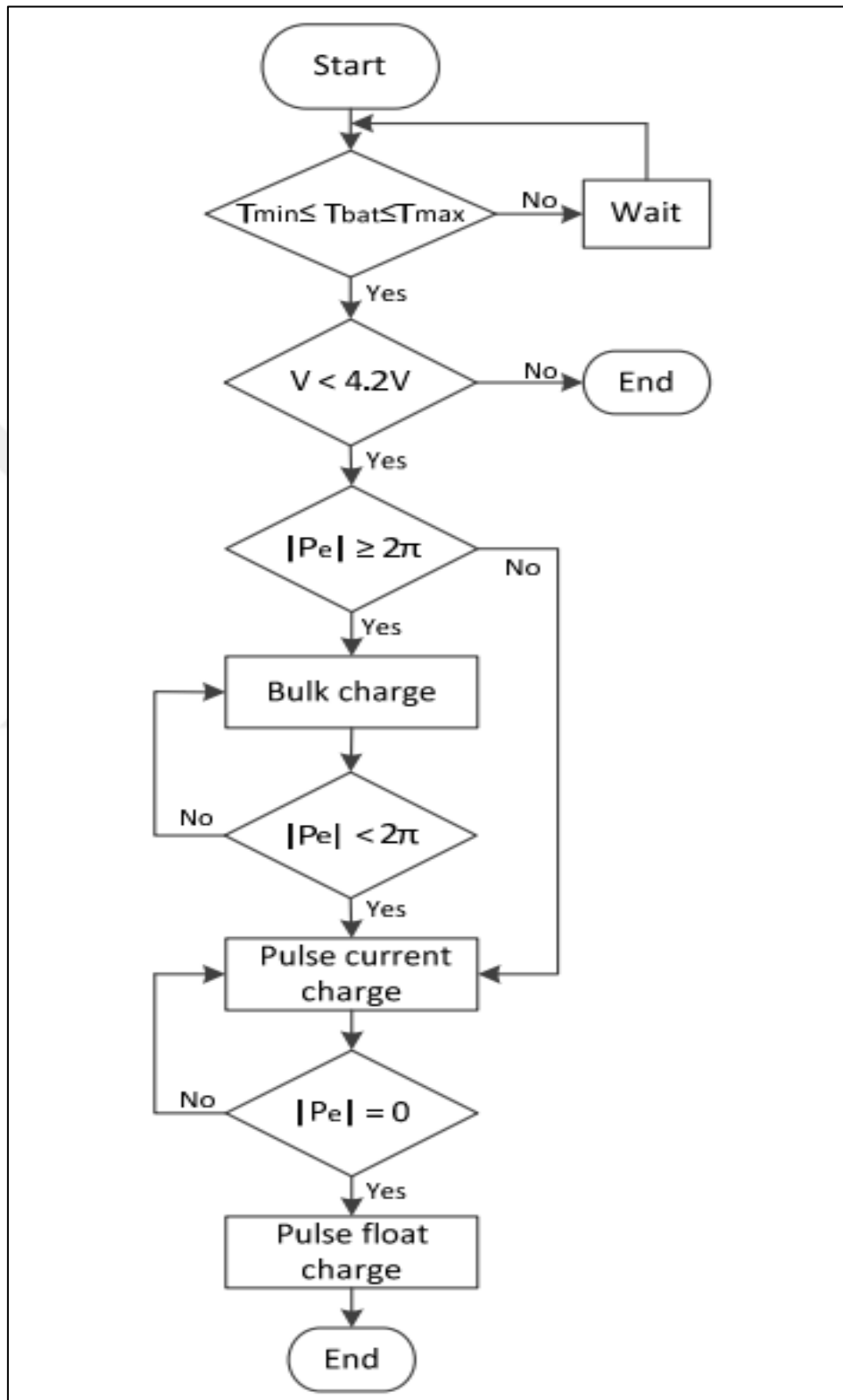


Figure 2.11: Flowchart illustrating the process of charging the PLL- CC/CV.

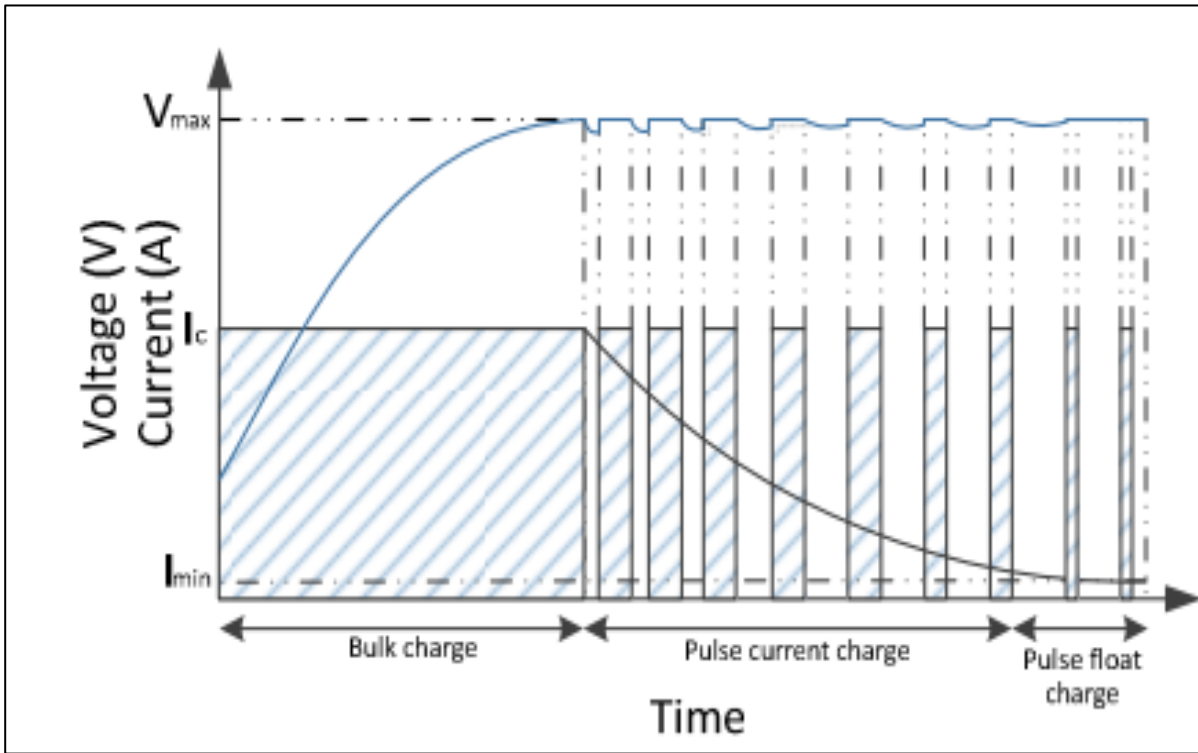


Figure 2.12: Displaying the charging pattern of the IPPL-CC/CV.

3. METHODOLOGY

In this work proposed Li-ion battery charger designed to work in two modes: constant charging current mode and constant voltage mode based on charge value battery state. This proposed charger tracks MPP for PV array and charge the battery in the suitable manner. as presented in figure below (Fig. 3.1), shows the overall system Simulink model.

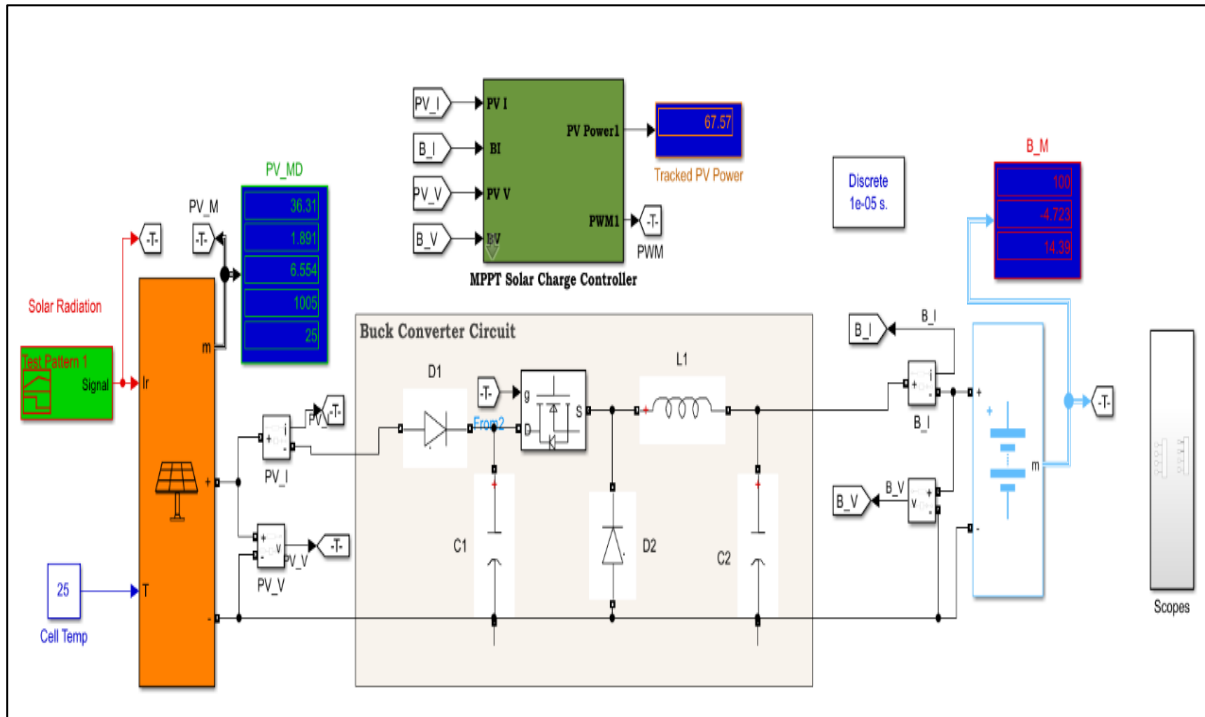


Figure 3.1: Proposed system Simulink model.

3.1 SYSTEM COMPONENTS

The proposed system contains four main parts: PV array, DC/DC buck converter, Battery and MPPT controller.

3.1.1 PV Array

PV array specification are listed in table 3.1 and the MPP test for the PV array is shown in figure below (Fig 3.2).

Table 3.1: PV array data.

Parallel strings	1	Isc (A)	8.46
Series connected modules	1	V max. power (V)	30.2
Module	Canadian Solar Inc. CS6P-240P	I max. power (A)	7.95
Max. power (W)	240.09	Temperature coefficient of Voc (%/deg.C)	-0.35
Cells/Module (Ncells)	60	Temperature coefficient of Isc (%/deg.C)	0.04
Voc (V)	37.3		

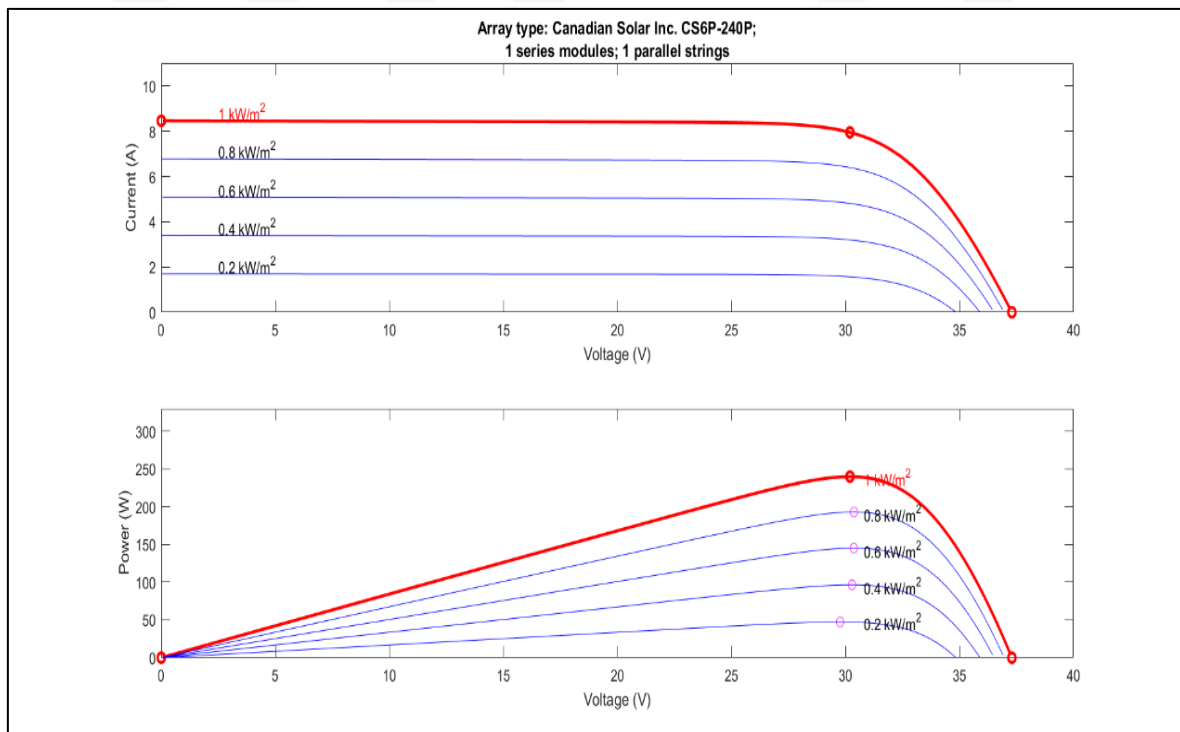


Figure 3.2: PV array P-V & I-V curves.

3.1.2 DC/DC Converter

A DC/DC buck converter is used to track the MPP and to make the PV array voltage suitable for battery charging. The buck converter Simulink model is shown in figure below (Fig. 3.3) and its parameters are listed in Table 3.2.

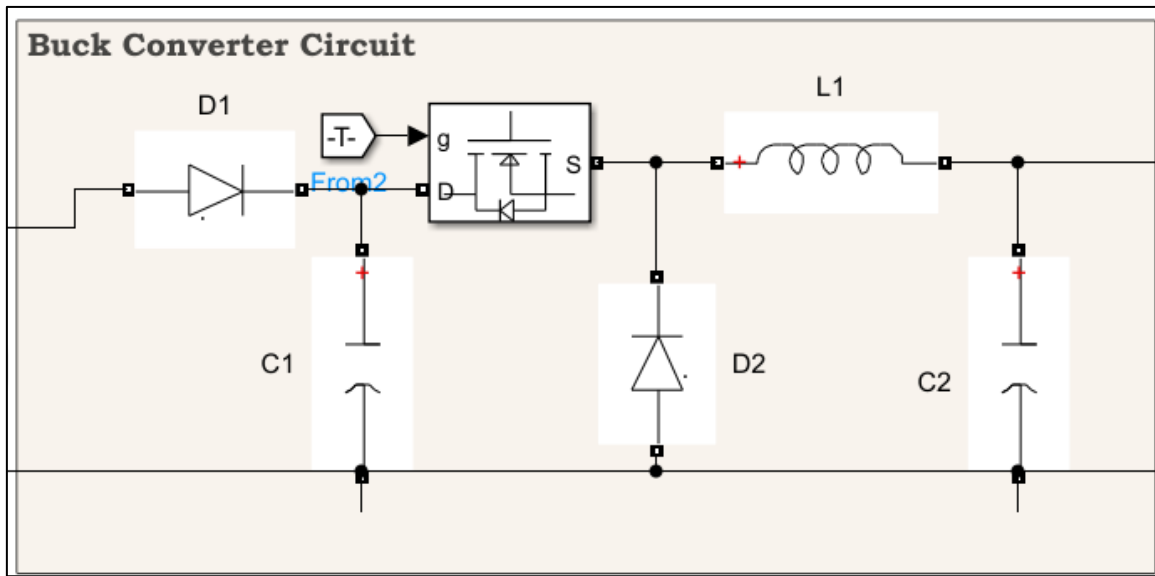


Figure 3.3: DC/DC buck converter Simulink model.

Table 3.2: Buck converter parameters

D1,D2	C1,C2	Q1	L1
Diode	1000 uF	MOSFET	10 mH

3.1.3 MPPT And Control

The MPPT and control block contains the MPPT algorithm, this algorithm track the MPP and in same time control the battery charging process. The charging starts in constant current CCCM and when the battery charge reaches an specific value the charging mode change to constant voltage charging mode CVCN, this charging strategy keep the battery save and also prevent the overloading on PV array when the battery is empty and need to be charged. Figure below (Fig. 3.4) shows the MPPT and control block.

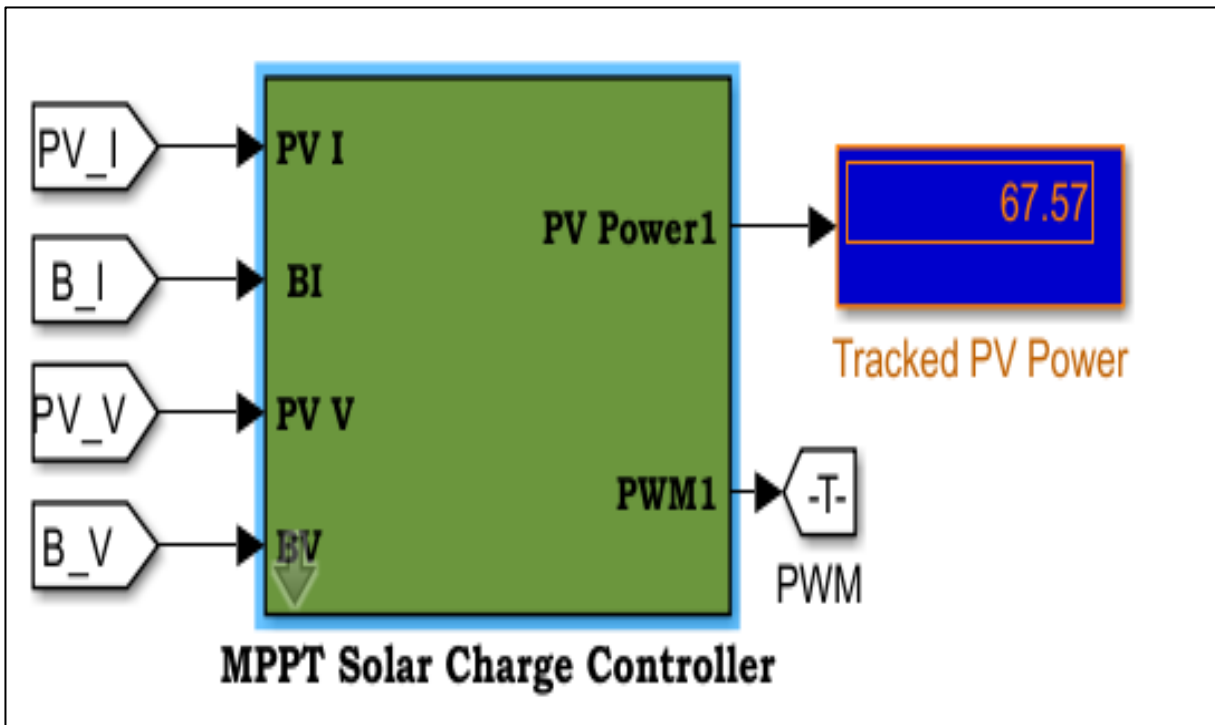


Figure 3.4: MPPT and control block.

The control algorithm is listed below:

```
function [D,PA] = fcn(VA,IA,VB,IB,Ta)
```

```
Nc = 6;
```

```
alpha = -0.0035;
```

```
VBmin = 12.7+((Ta-25)*Nc*alpha);
```

```
VBmax = 14.4+((Ta-25)*Nc*alpha);
```

```
C= 50;
```

```
IBmin = C/100;
```

```
ITrickle = 0.2;
```

```
Beta = 0.9;
```

```
DD = 1e-6;
```

persistent PAP VAP DP UP IBmax

if isempty(PAP)

 PAP = 0;

 VAP = 0;

 DP = 0;

 UP = 1;

 IBmax = C/5;

end

PA = VA*IA;

DPA = PA-PAP;

DVA = VA-VAP;

D = DP;

%%

if IB>IBmax

 UP = 0;

elseif VB>VBmax && IB<IBmax

 if IBmax>IBmin

 IBmax = Beta*IBmax;

 else

 IBmax = ITrickle;

 end

else

```
if VB<VBmax && IB<IBmax
```

```
    UP = 1;
```

```
end
```

```
if VB<VBmin
```

```
    IBmax = C/5;
```

```
end
```

```
end
```

```
if UP == 0
```

```
    D = DP-DD;
```

```
elseif UP == 1
```

```
    if DPA>0
```

```
        if DVA>0
```

```
            D = DP-DD;
```

```
        elseif DVA<0
```

```
            D = DP+DD;
```

```
        end
```

```
    elseif DPA<0
```

```
        if DVA>0
```

```
            D = DP+DD;
```

```
        elseif DVA<0
```

```
            D = DP-DD;
```

```
        end
```

```

end
end
if D>1
    D=1;
elseif D<0
    D=0;
end
DP = D;
PAP = PA;
VAP = VA;

```

3.1.4 Battery

A lithium-ion battery is used in this work. The battery specifications are listed in Table 3.3. The Li-ion battery selected because of its importance and widely use.

Table 3.3: Battery specifications

Battery type	Nominal voltage	Rated capacity (Ah)	Cut-off voltage (V)	Fully charged voltage (V)	Nominal discharge current (A)	Internal resistance (ohm)	Capacity at nominal voltage (Ah)
Li-ion	12	50	9	14.4	10	0.0024	10

Nominal current discharge curves are shown in figure below (Fig. 3.5).

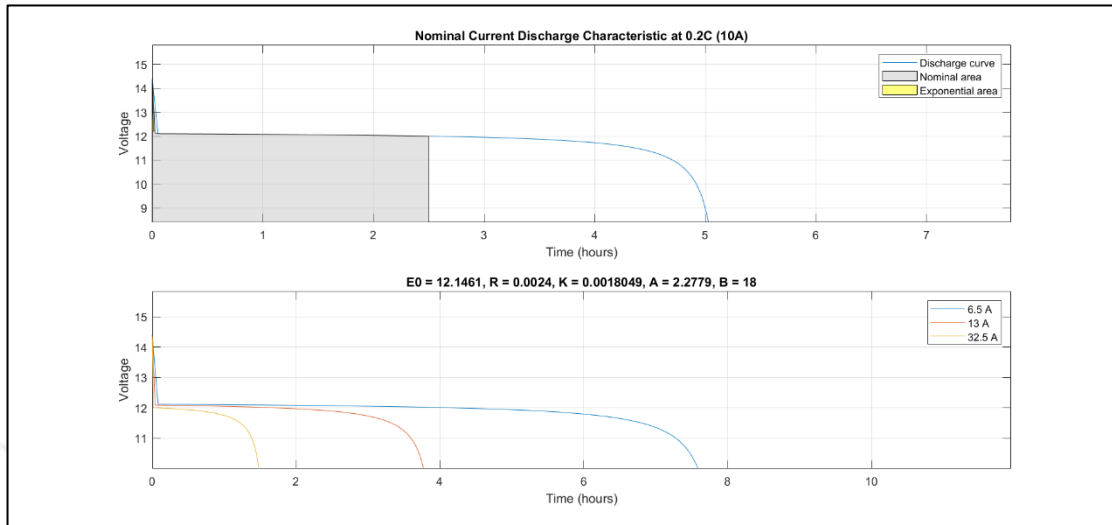


Figure 3.5: Nominal discharge current curves.

3.2 OPERATION MODES

The proposed battery charger works in two operation modes: constant charging mode and constant charging voltage.

3.2.1 Constant Current Charging Mode

Constant current charging is a basic method that only requires a current level of around 10% of the maximum battery rating. In addition to the inconvenience of a lengthy charge period, overcharging a battery may cause it to overheat and shorten its lifespan, necessitating an early battery replacement. The use of this technique is appropriate for many types of batteries. Once charged, the battery should be removed, or a timer feature employed.

3.2.2 Constant Voltage Charging Mode

In a constant-voltage charger, the battery receives the entire current output of the charger until the power source reaches the target voltage. When the threshold voltage is achieved, the current will gradually decrease to a minimal amount. Keep the battery connected to the charger until it's time to use it, and it will maintain its "float voltage," slowly charging to make up for the battery's natural rate of self-discharge.

4. SIMULATION RESULTS

The proposed system simulated for two operating cases, the first case when the solar irradiance is constant (1000 W/m^2) and the second case when the solar irradiance varied from minimum to maximum value.

4.1 CONSTANT IRRADIANCE CASE

4.1.1 System Performance in Case Of 1000 W/m^2

The charging in this case starts with CC charging mode and change to CV charging mode. The battery and PV array voltage and current curves are shown in figure below (Fig. 4.1).

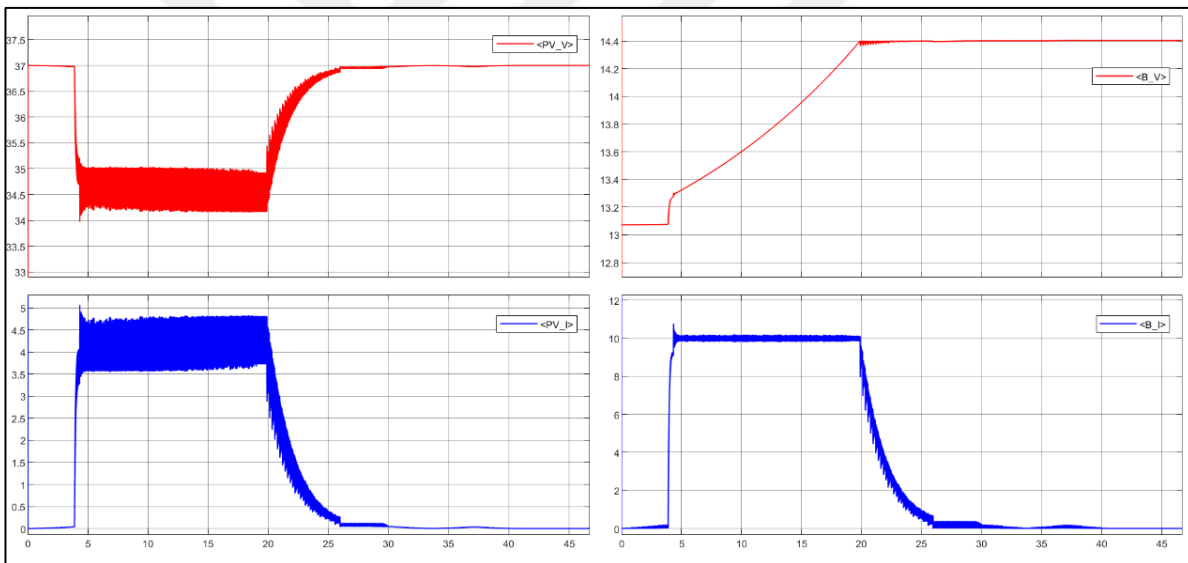


Figure 4.1: PV and battery voltage and current curves.

The system performs a high performance in this operating mode, the system efficiency along the simulation interval is near 95% as shown in figure below (Fig. 4.2). In this operation mode the MPPT system tracks the PV maximum power until the battery reaches the constant voltage charging mode in this point the tracked power is that the power required to charge the battery in the constant voltage mode and decrease until reaches the zero when the battery fully charged.

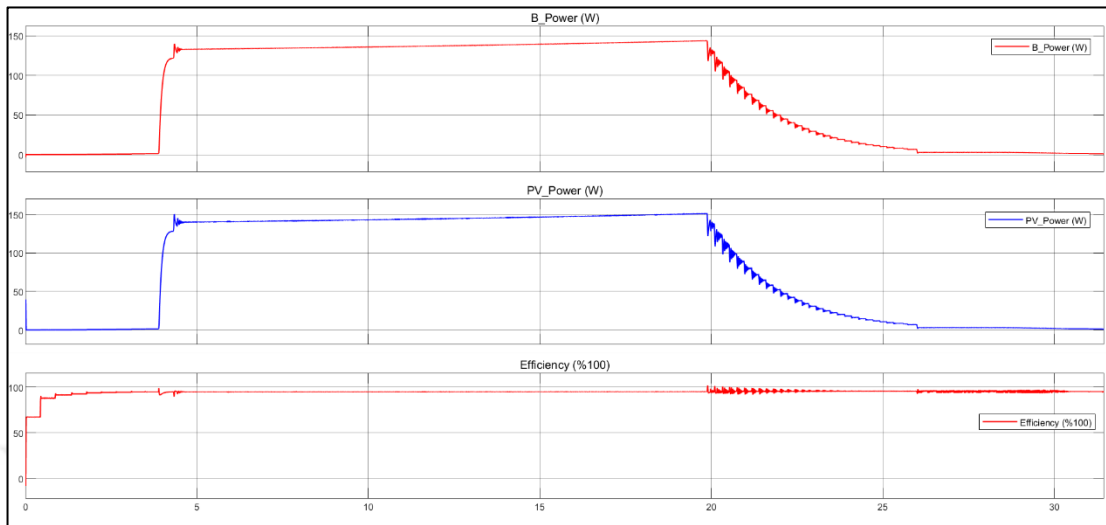


Figure 4.2: System efficiency.

4.1.2 System Performance in Case Of 200 W/m²

The system voltage and current curves are shown in figure below in (Fig. 4.3), the time to need by the battery to be fully charged is about 70 second. The battery charging current in CC duty is not 100% constant but varied between 2 and 4 amperes depending on the PV array current which is low in low irradiance level.

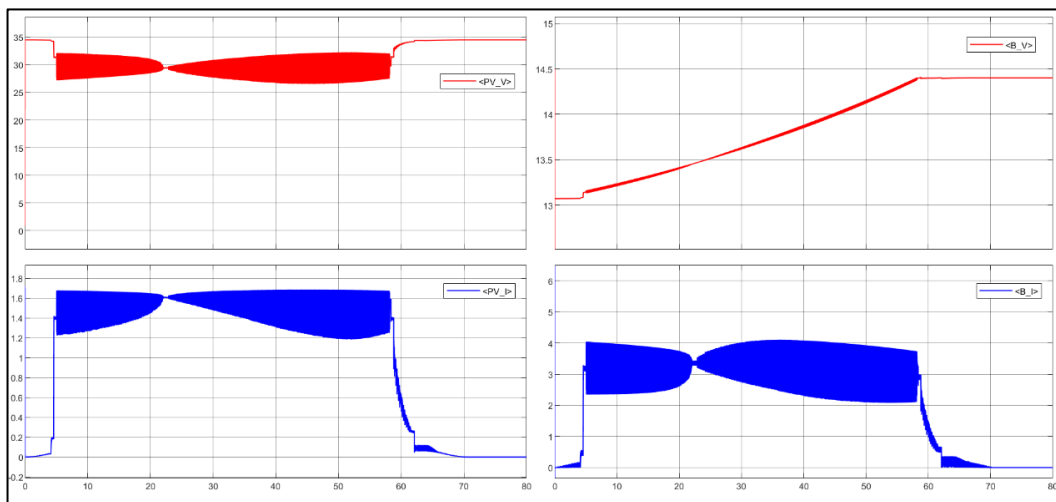


Figure 4.3: Battery and PV V&I curves in case of 200 W/m².

The P-V and I-V curves are shown in figure below (Fig. 4.4), in case of 200 W/m², it is shown that the charging power is the maximum power until the battery enter the CV charging mode.

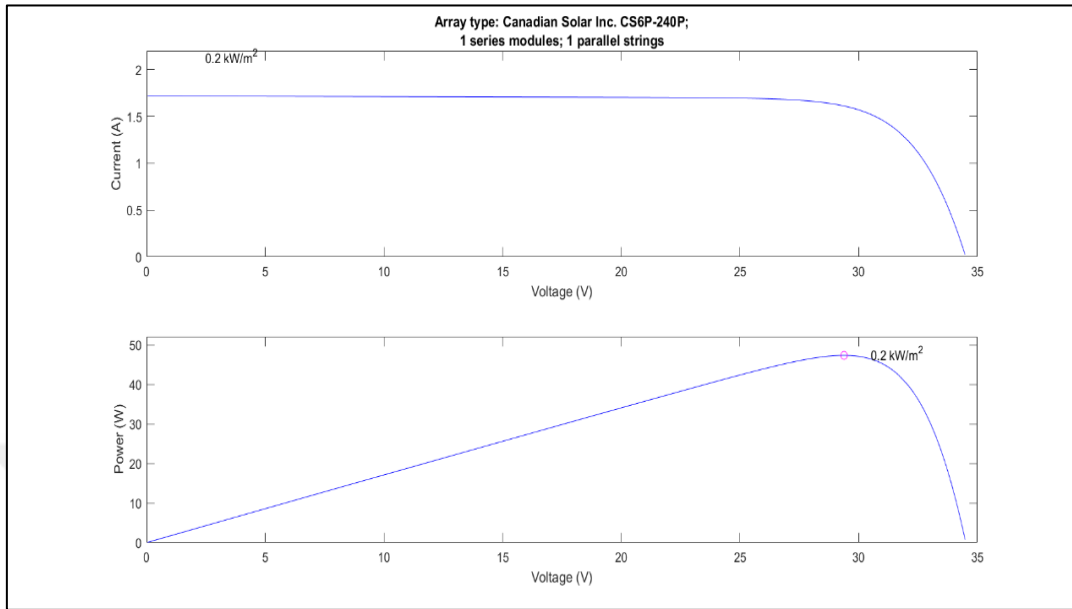


Figure 4.4: P-V & I-V curves for the PV array in case of 200 W/m^2 .

4.1.3 System Performance in Case Of 400 W/m^2

In this case the solar irradiance still constant in 400 W/m^2 level. The charging time decreases to 45 second as shown in figure 4.5. The system power and efficiency curves are shown in figure 4.6, it is clear that the system efficiency is near 95% until the fully charge state reached.

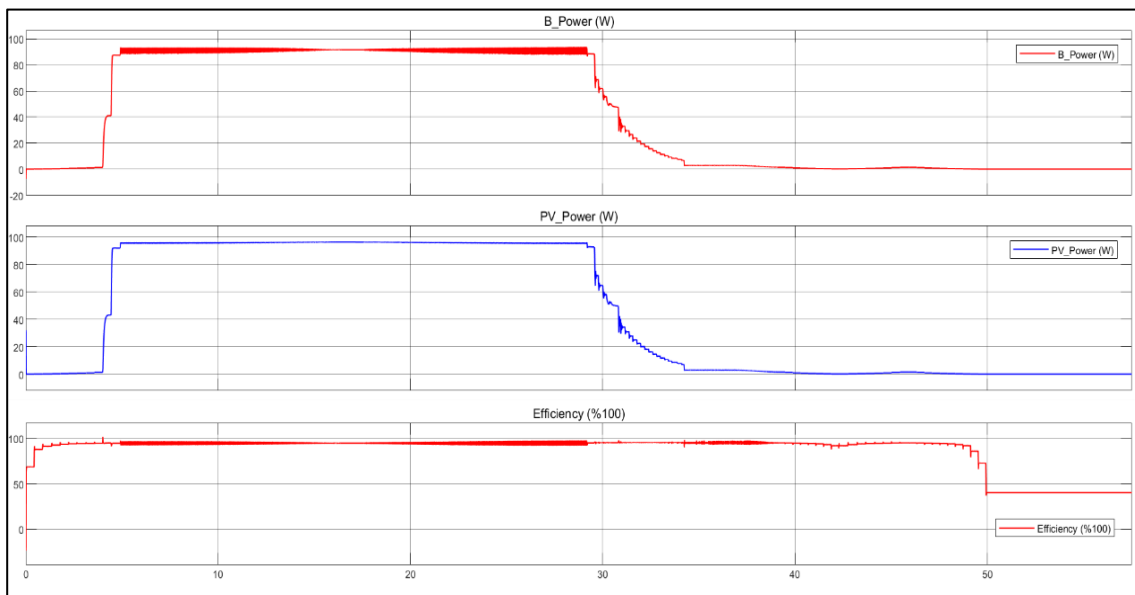


Figure 4.5: System power and efficiency curves in case of 400 W/m^2 .

The P-V and I-V curves of the PV array in case of 400 W/m² are shown in figure 4.6 to show if the system works in maximum power point.

From (Fig. 4.5) and (Fig. 4.6) it is clear that the system works in maximum power which is 96 watt.

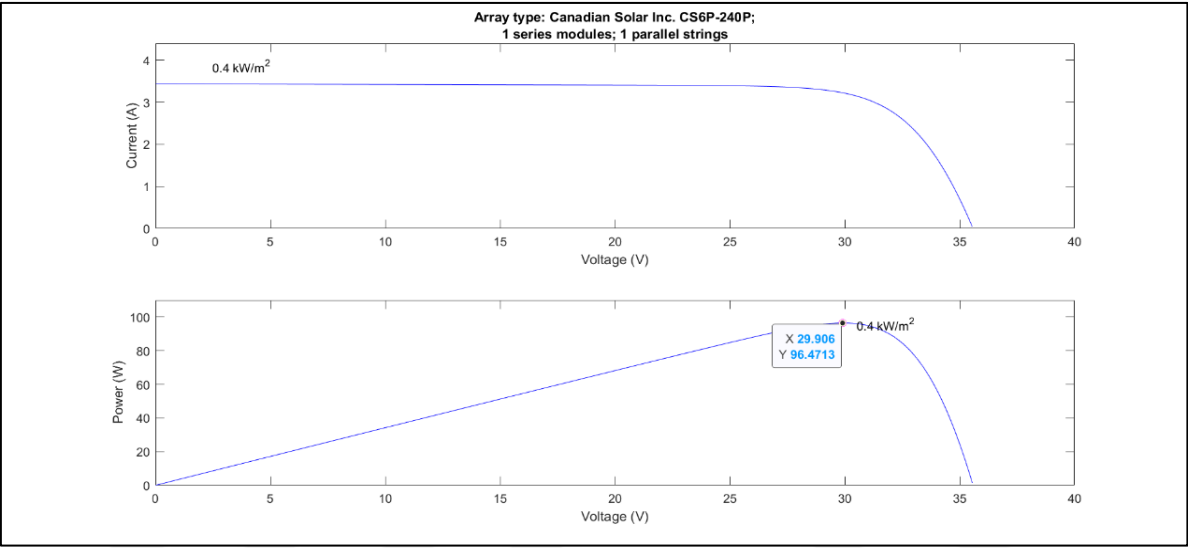


Figure 4.6: PV array P-V & I-V curves in case of 400 W/m².

4.1.4 System Performance in Case Of 600 W/m²

In this case the solar irradiance is fixed (600 W/m²), system voltage curves are shown in figure below (Fig. 4.7), from this figure inspection the charging time reduced to 35 second.

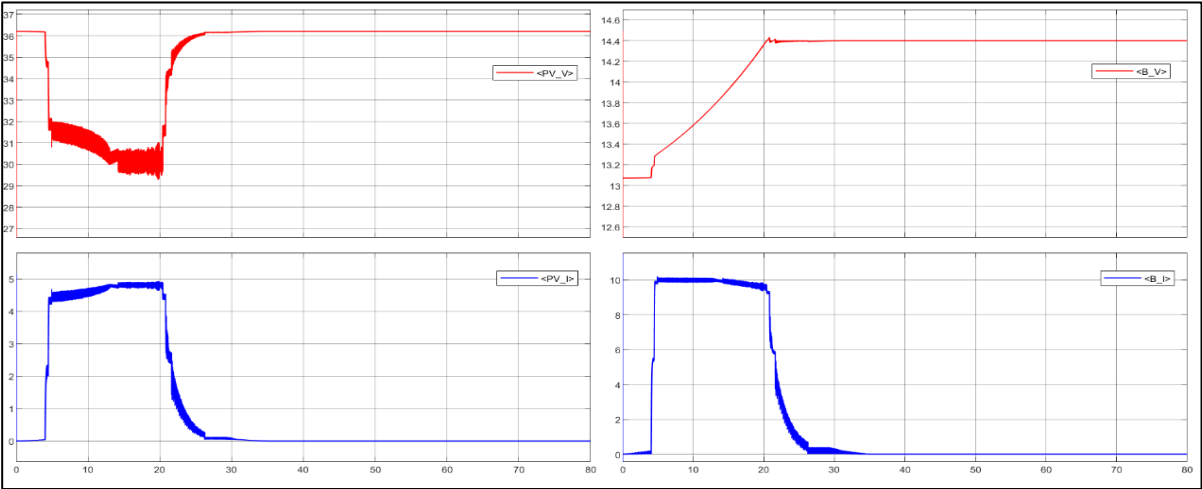


Figure 4.7: System voltage and current curves in case of 600 W/m².

The system power and efficiency curves are shown in figure below (Fig. 4.8), the system efficiency still near 95% until full charge case reached.

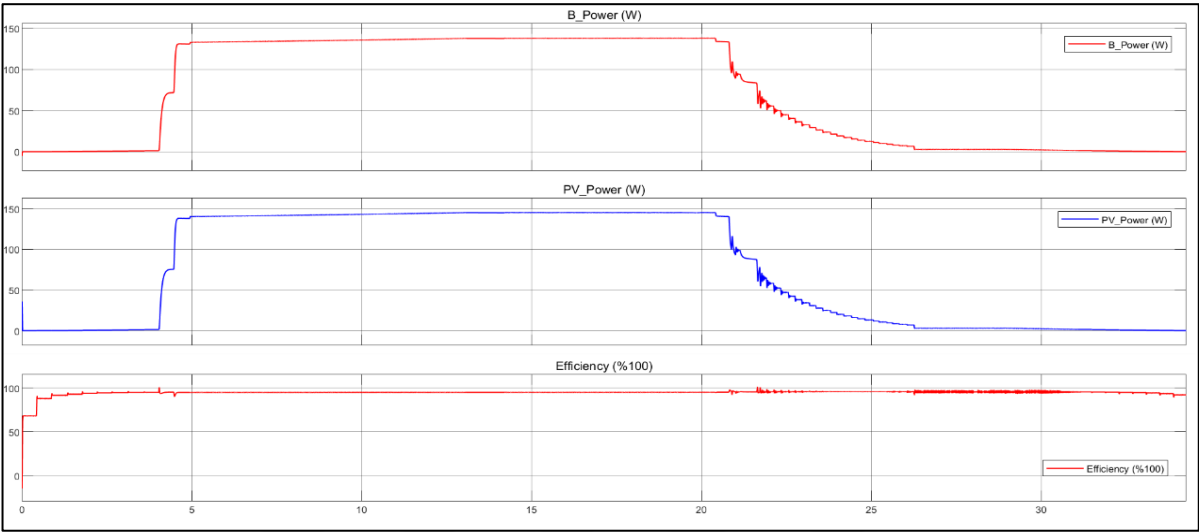


Figure 4.8: System power and efficiency curves in case of 600 W/m²

To check if the system works in MPP it is required to compare the P-V curve with the system power, P-V and I-V curves are shown in figure below (Fig. 4.9).

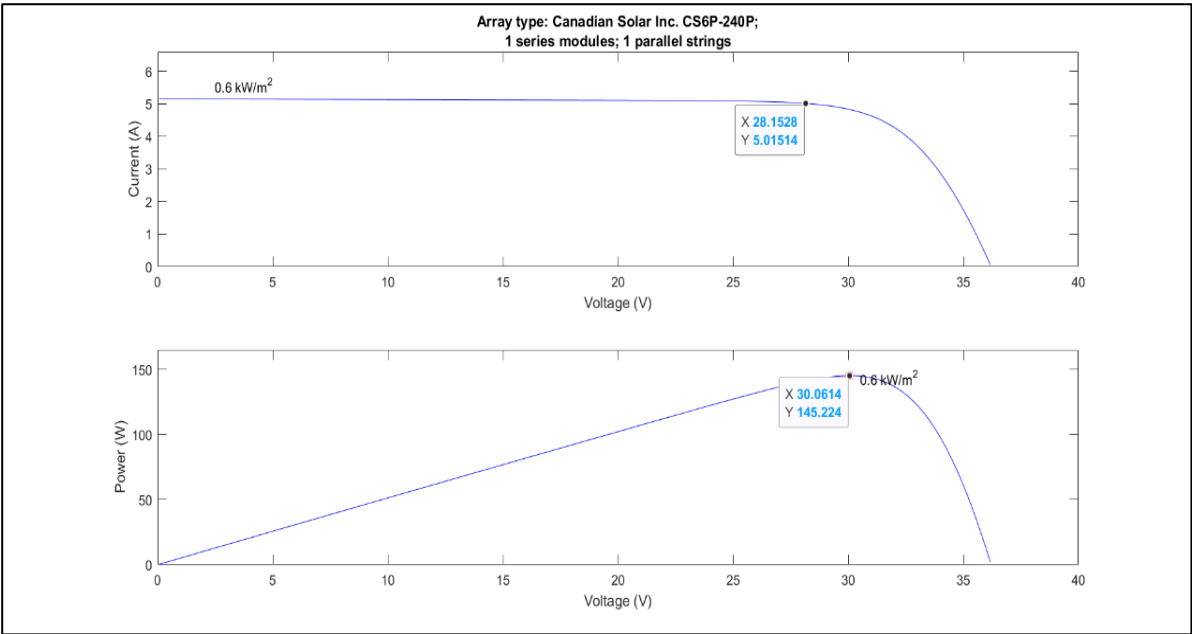


Figure 4.9: PV array P-V & I-V curves in case of 600 W/m²

Comparing the system charging power which is 145 watt and it the same maximum power.

4.1.5 System Performance in Case Of 800 W/m²

The system performance in case of 800 W/m² such is system voltage and power curves shown in below figure (Fig. 4.10), and System efficiency shown in (Fig. 4.11).

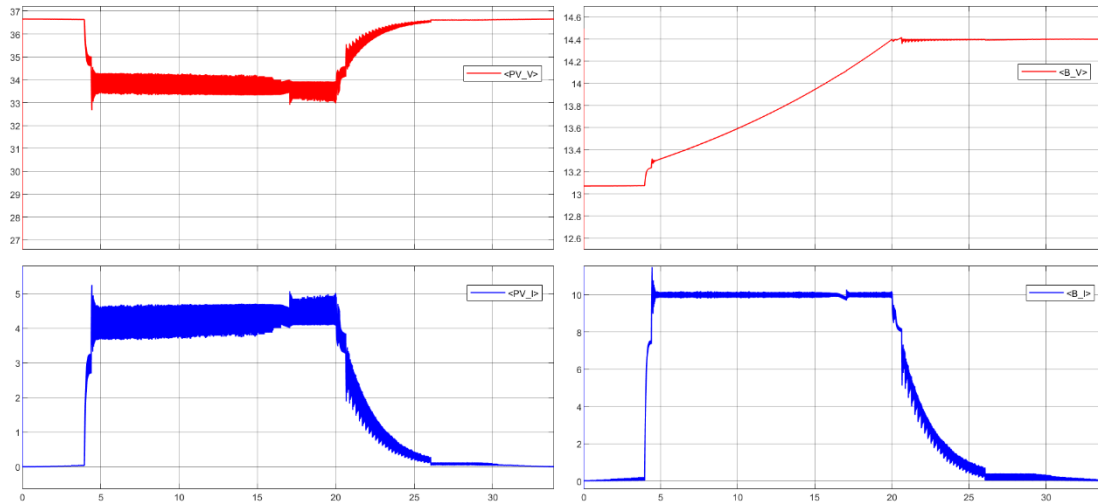


Figure 4.10: System voltage and power curves in case of 800 W/m²

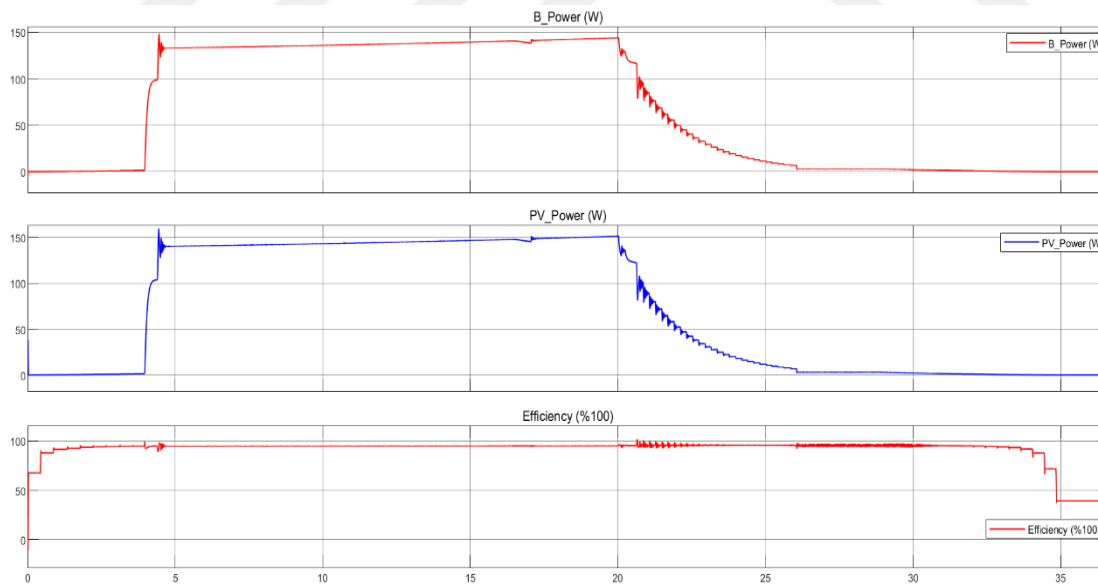


Figure 4.11: System efficiency in case of 800 W/m²

To proof the system working in MPP it is required to plot P-V and I-V curves of the PV array in 800 W/m² irradiance level, shown in figure below (Fig. 4.12).

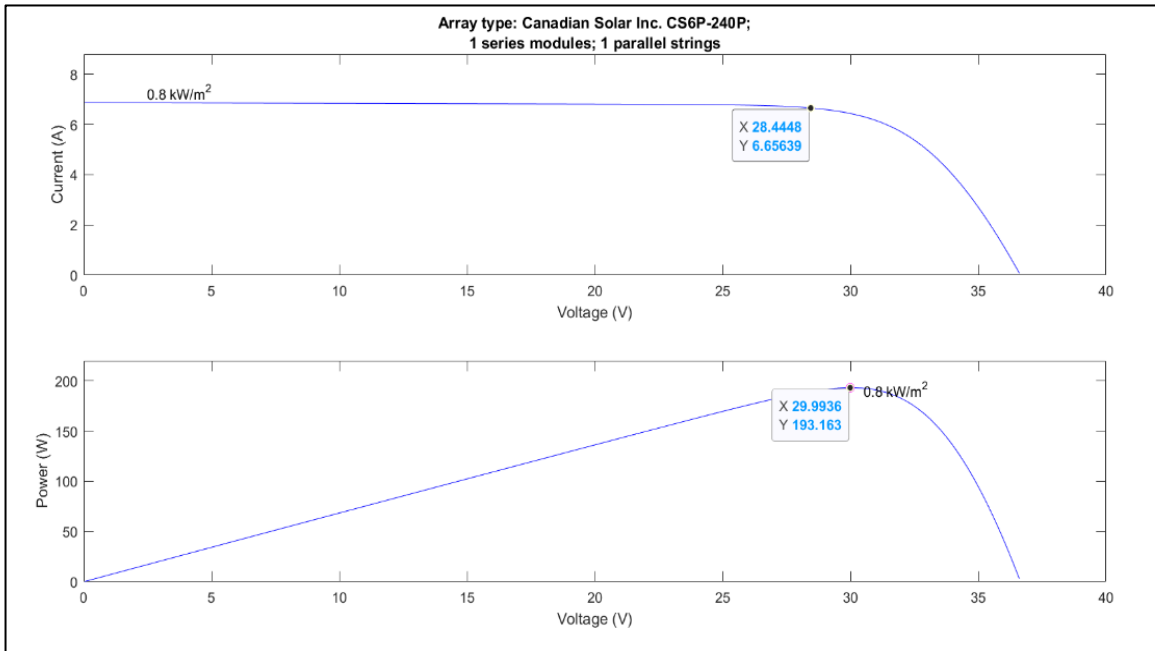


Figure 4.12: PV array P-V & I-V curves in case of 800 W/m².

4.2 VARIABLE IRRADIANCE OPERATING MODE

In this mode the irradiance level varied from minimum value to reach the maximum value (1000 W/m²). In (Fig. 4.13) shows the voltage and current curves for both battery and PV array curves in this operating mode.

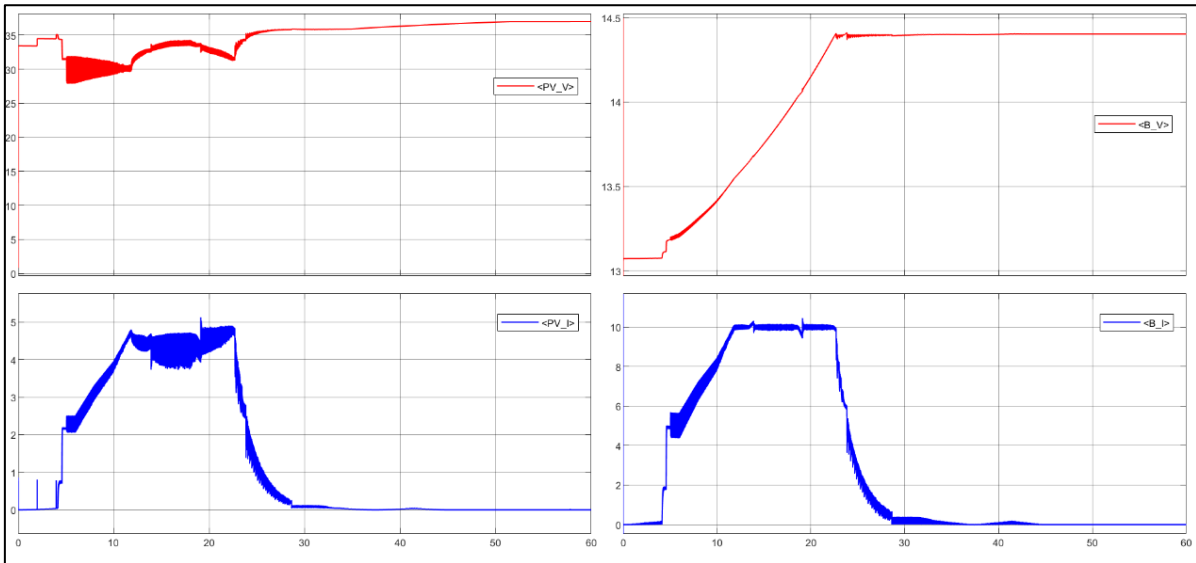


Figure 4.13: System voltage and power curves in case of variable irradiance.

The efficiency curve for the system is shown in (Fig. 4.14), it is clear that the system efficiency still near 100% until the battery reached full charge the efficiency decreases because the battery can not store the total PV array power.

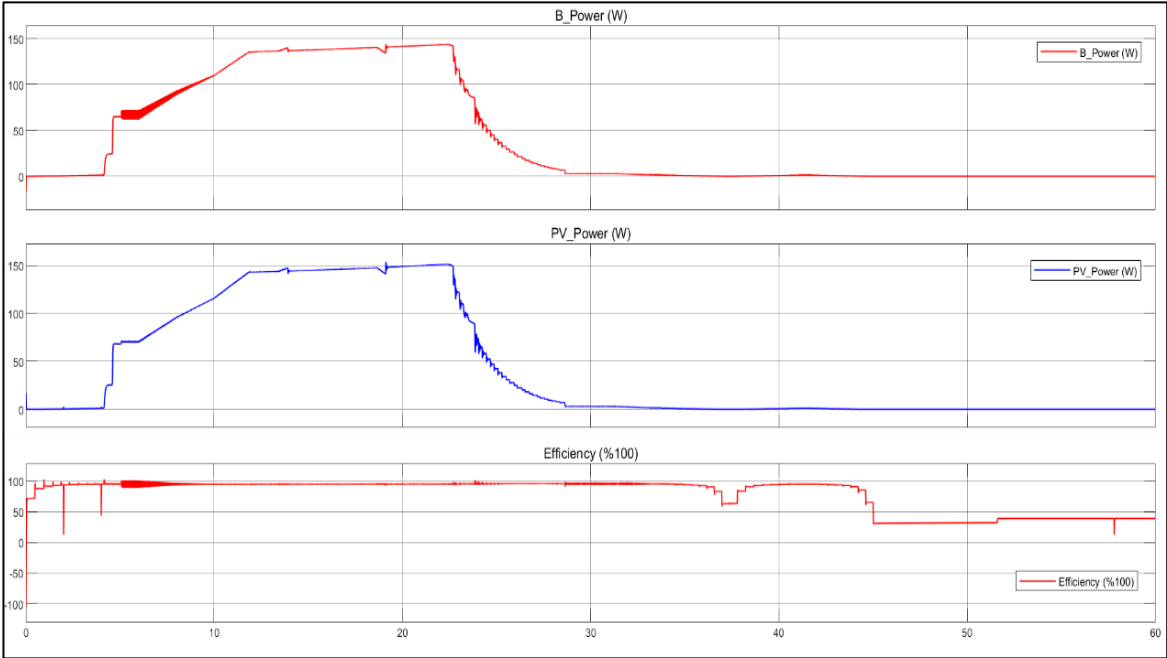


Figure 4.14: System efficiency in case of variable irradiance.

5. CONCLUSION AND FUTURE WORKS

5.1 CONCLUSIONS

The Li-ion battery charger based on PV array power source designed and simulated for all expected operating cases, for fixed irradiance level from 200 – 1000 W/m² for each case. In all studied cases the system works in high efficiency. The proposed battery charger works in CC/CV charging procedure to keep the battery safe in charging state period (when the battery is empty) and also to save the PV array system from overloading.

The system efficiency in all cases higher than or equal to 95%. The system works in MPP for all cases until the battery reaches fully charged case, the system works in less than the MPP depending on the charging power required by the battery.

The PV array-based battery charger can perform two tasks in the same time (MPPT and CC/CV charging process).

5.2 FUTURE WORKS

- a. Include the battery charger within PV powered system to ensure that there is no unused power when the battery reaches the fully charge state.
- b. Modify the control algorithm to stop control the charging time (fast charging process).
- c. Implement the proposed system using suitable components as a prototype model and compare the simulation results with the experimental results.
- d. Use the same charging system with other battery type.

REFERENCES

- [1] D. Andrea, "Battery management systems for large lithium-ion battery packs." Artech house, 2010.
- [2] G. L. B. Market, "Market 2011-2015," *Int. J. Econ. Res.*, vol. 3, no. 1, pp. 1–8, 2012.
- [3] P. Jover Almirall, "Lithium-ion batteries performance optimization for vehicle-to-grid (V2G) integration in the smart grid." Universitat Politècnica de Catalunya, 2017.
- [4] A. W. Saffar, "Battery Charge Control for Standalone PV System by Using Matlab/Simulink." 2021.
- [5] J. Jana, K. Das Bhattacharya, and H. Saha, "Design & implementation of MPPT algorithm for battery charging with photovoltaic panel using FPGA," in 2014 6th IEEE Power India International Conference (PIICON), 2014, pp. 1–5.
- [6] M. Pastre et al., "A solar battery charger with maximum power point tracking," in 2011 18th IEEE International Conference on Electronics, Circuits, and Systems, 2011, pp. 394–397.
- [7] S. Armstrong, M. E. Glavin, and W. G. Hurley, "Comparison of battery charging algorithms for stand alone photovoltaic systems," in 2008 IEEE Power Electronics Specialists Conference, 2008, pp. 1469–1475.
- [8] S. Padhee, U. C. Pati, and K. Mahapatra, "Design of photovoltaic MPPT based charger for lead-acid batteries," in 2016 IEEE International Conference on Emerging Technologies and Innovative Business Practices for the Transformation of Societies (EmergiTech), 2016, pp. 351–356.
- [9] W. Chen, M. Cai, X. Tan, and B. Wei, "Parameter identification and state-of-charge estimation for li-ion batteries using an improved tree seed algorithm," *IEICE Trans. Inf. Syst.*, vol. 102, no. 8, pp. 1489–1497, 2019.
- [10] C. R. Birkl, M. R. Roberts, E. McTurk, P. G. Bruce, and D. A. Howey, "Degradation diagnostics for lithium ion cells," *J. Power Sources*, vol. 341, pp. 373–386, 2017.

- [11] J. Wehbe and N. Karami, "Battery equivalent circuits and brief summary of components value determination of lithium ion: A review," in 2015 Third International Conference on Technological Advances in Electrical, Electronics and Computer Engineering (TAEECE), 2015, pp. 45–49.
- [12] B. Xia, H. Wang, Y. Tian, M. Wang, W. Sun, and Z. Xu, "State of charge estimation of lithium-ion batteries using an adaptive cubature Kalman filter," *Energies*, vol. 8, no. 6, pp. 5916–5936, 2015.
- [13] C. Zhang, K. Li, L. Pei, and C. Zhu, "An integrated approach for real-time model-based state-of-charge estimation of lithium-ion batteries," *J. Power Sources*, vol. 283, pp. 24–36, 2015.
- [14] D. Cui et al., "A novel intelligent method for the state of charge estimation of lithium-ion batteries using a discrete wavelet transform-based wavelet neural network," *Energies*, vol. 11, no. 4, p. 995, 2018.
- [15] R. Velho, M. Beirão, M. D. R. Calado, J. Pombo, J. Fermeiro, and S. Mariano, "Management system for large li-ion battery packs with a new adaptive multistage charging method," *Energies*, vol. 10, no. 5, p. 605, 2017.
- [16] H. Popp, J. Attia, F. Delcorso, and A. Trifonova, "Lifetime analysis of four different lithium ion batteries for (plug-in) electric vehicle," 2014.
- [17] J. Cao, N. Schofield, and A. Emadi, "Battery balancing methods: A comprehensive review," in 2008 IEEE Vehicle Power and Propulsion Conference, 2008, pp. 1–6.
- [18] I. Aizpuru, U. Iraola, J. M. Canales, M. Echeverria, and I. Gil, "Passive balancing design for Li-ion battery packs based on single cell experimental tests for a CCCV charging mode," in 2013 International Conference on Clean Electrical Power (ICCEP), 2013, pp. 93–98.
- [19] M. Einhorn, W. Roessler, and J. Fleig, "Improved performance of serially connected Li-ion batteries with active cell balancing in electric vehicles," *IEEE Trans. Veh. Technol.*, vol. 60, no. 6, pp. 2448–2457, 2011.

- [20] M. A. K. A. Biabani and F. Ahmed, "Maximum power point tracking of photovoltaic panels using perturbation and observation method and fuzzy logic control based method," in 2016 International Conference on Electrical, Electronics, and Optimization Techniques (ICEEOT), 2016, pp. 1614–1620.
- [21] R. Li, X. Wei, H. Sun, H. Sun, and X. Zhang, "Fast Charging Optimization for Lithium-Ion Batteries Based on Improved Electro-Thermal Coupling Model," *Energies*, vol. 15, no. 19, p. 7038, 2022.
- [22] Ö. Yasemin, "A NEW CONTROLLER FOR PHOTOVOLTAIC PANEL FED UNIFIED POWER QUALITY CONDITIONER TO POWER QUALITY IMPROVEMENT," *Mugla J. Sci. Technol.*, vol. 7, no. 1, pp. 14–24.
- [23] Kr. Rao and K. S. Srikanth, "Improvement of power quality using fuzzy logic controller in grid connected photovoltaic cell using UPQC," *Int. J. Power Electron. Drive Syst.*, vol. 5, no. 1, p. 101, 2014.
- [24] F. Palmiro, R. Rayudu, and R. Ford, "Modelling and simulation of a solar PV lithium ion battery charger for energy kiosks application," in 2015 IEEE PES Asia-Pacific Power and Energy Engineering Conference (APPEEC), 2015, pp. 1–5.
- [25] J. Ahmad, "A fractional open circuit voltage based maximum power point tracker for photovoltaic arrays," in 2010 2nd International Conference on Software Technology and Engineering, 2010, vol. 1, pp. V1-247.
- [26] R. J. Brodd, A. Kozawa, and M. Yoshio, *Lithium-Ion Batteries: Science and Technologies*. Springer, 2009.
- [27] J. Mindemark, M. J. Lacey, T. Bowden, and D. Brandell, "Beyond PEO—Alternative host materials for Li⁺-conducting solid polymer electrolytes," *Prog. Polym. Sci.*, vol. 81, pp. 114–143, 2018.
- [28] Y. Li, Y. Lu, P. Adelhelm, M.-M. Titirici, and Y.-S. Hu, "Intercalation chemistry of graphite: alkali metal ions and beyond," *Chem. Soc. Rev.*, vol. 48, no. 17, pp. 4655–4687, 2019.

- [29] M. Watanabe, K. Dokko, K. Ueno, and M. L. Thomas, "From ionic liquids to solvate ionic liquids: challenges and opportunities for next generation battery electrolytes," *Bull. Chem. Soc. Jpn.*, vol. 91, no. 11, pp. 1660–1682, 2018.
- [30] W. Shen, T. T. Vo, and A. Kapoor, "Charging algorithms of lithium-ion batteries: An overview," in *2012 7th IEEE conference on industrial electronics and applications (ICIEA)*, 2012, pp. 1567–1572.
- [31] T. T. Vo, W. Shen, and A. Kapoor, "Experimental comparison of charging algorithms for a lithium-ion battery," in *2012 10th International Power & Energy Conference (IPEC)*, 2012, pp. 207–212.
- [32] M. Di Yin, J. Cho, and D. Park, "Pulse-based fast battery IoT charger using dynamic frequency and duty control techniques based on multi-sensing of polarization curve," *Energies*, vol. 9, no. 3, 2016.
- [33] J. M. Amanor-Boadu, M. A. Abouzied, and E. Sánchez-Sinencio, "An efficient and fast li-ion battery charging system using energy harvesting or conventional sources," *IEEE Trans. Ind. Electron.*, vol. 65, no. 9, pp. 7383–7394, 2018.
- [34] J. M. Amanor-Boadu, A. Guiseppi-Elie, and E. Sánchez-Sinencio, "Search for optimal pulse charging parameters for Li-ion polymer batteries using Taguchi orthogonal arrays," *IEEE Trans. Ind. Electron.*, vol. 65, no. 11, pp. 8982–8992, 2018.
- [35] D. R. Ely and R. E. García, "Heterogeneous nucleation and growth of lithium electrodeposits on negative electrodes," *J. Electrochem. Soc.*, vol. 160, no. 4, p. A662, 2013.
- [36] A. A.-H. Hussein and I. Batarseh, "A review of charging algorithms for nickel and lithium battery chargers," *IEEE Trans. Veh. Technol.*, vol. 60, no. 3, pp. 830–838, 2011.
- [37] G.-C. Hsieh, L.-R. Chen, and K.-S. Huang, "Fuzzy-controlled Li-ion battery charge system with active state-of-charge controller," *IEEE Trans. Ind. Electron.*, vol. 48, no. 3, pp. 585–593, 2001.

- [38] L.-R. Chen, R. C. Hsu, and C.-S. Liu, "A design of a grey-predicted Li-ion battery charge system," *IEEE Trans. Ind. Electron.*, vol. 55, no. 10, pp. 3692–3701, 2008.
- [39] L.-R. Chen, "PLL-based battery charge circuit topology," *IEEE Trans. Ind. Electron.*, vol. 51, no. 6, pp. 1344–1346, 2004.
- [40] L.-R. Chen, J.-J. Chen, N.-Y. Chu, and G.-Y. Han, "Current-pumped battery charger," *IEEE Trans. Ind. Electron.*, vol. 55, no. 6, pp. 2482–2488, 2008.

